nature reviews physics

https://doi.org/10.1038/s42254-024-00748-7

Review article

Check for updates

Single-molecule FRET for probing nanoscale biomolecular dynamics

Daniel Nettels [1] ✉, Nicola Galvanetto [1,2], Miloš T. Ivanović [1], Mark Nüesch [1], Tianjin Yang [1] & Benjamin Schuler [1,2] ✉

Abstract

Single-molecule spectroscopy is a powerful method for studying the physics of molecular systems, particularly biomolecules, such as proteins and nucleic acids. By avoiding ensemble averaging, single-molecule techniques can resolve structural distributions and fluctuations even for complex and conformationally heterogeneous systems; they also reveal the close link between biological function and the statistical mechanics of the underlying processes. The combination of single-molecule fluorescence detection with Förster resonance energy transfer has become an essential tool for probing biomolecular dynamics on timescales ranging from nanoseconds to days. This Review briefly outlines the state of the art of single-molecule Förster resonance energy transfer spectroscopy and then highlights some of the most important physics-based developments that are expected to further expand the scope of the technique. Key areas of progress include improved time resolution, access to nonequilibrium dynamics and synergies with advances in data analysis and simulations. These developments create new opportunities for attaining a comprehensive understanding of the dynamics and functional mechanisms of biological processes at the nanoscale.

Sections

[1]Department of Biochemistry, University of Zurich, Zurich, Switzerland. [2]Department of Physics, University of Zurich, Zurich, Switzerland. ✉e-mail: nettels@bioc.uzh.ch; schuler@bioc.uzh.ch

Key points

- The functions of biological macromolecules depend on changes in their conformations across 24 orders of magnitude in time.
- Single-molecule Förster resonance energy transfer can be used to probe biomolecular dynamics on nanometre-length scales across timescales from nanoseconds to days.
- An important challenge is to increase the time resolution for measurements of rapid dynamics and nonequilibrium processes.
- Nanophotonics, microfluidic mixing and advances in data analysis and molecular simulations are particularly promising strategies for extending the scope of single-molecule Förster resonance energy transfer.

Introduction

The complexity of living organisms is remarkably difficult to comprehend in its entirety. However, at the level of the individual biological macromolecules, there has been tremendous progress in the understanding of the physical mechanisms that enable their diverse functions. Advances in X-ray diffraction and its application to nucleic acids and proteins in the 1950s triggered a revolution in biology because it allowed the details of their 3D structures to be elucidated with Ångström resolution[1]. This information has been central to uncovering the inner workings of these remarkable molecular machines that ultimately underlie virtually all biological functions, which range from information storage and reproduction to chemical catalysis, molecular transport, cellular signal processing and cognition. On the basis of the structures of approximately 10^5 biological macromolecules experimentally determined to date[2] and the enormous amount of DNA sequence information gathered over the past 20 years[3], recent advances in machine learning[4] now provide us with a virtually complete protein structure inventory of life as we know it.

However, although many aspects of biomolecular function can be conjectured from these structural models, molecular function almost invariably requires molecular motion[5–7]. Classical examples include the changes in the structure of enzymes going through their cycles of catalysis; of membrane proteins as they enable transport of ions or molecules across lipid bilayers; or of large assemblies of proteins and nucleic acids involved in the replication of DNA or the synthesis of new proteins[8]. Similarly, the formation of the well-defined 3D structures of many proteins and nucleic acids requires the process of folding[9,10] that starts from a linear chain of amino acids or nucleotides. Additionally, more than half of all human proteins contain large regions that do not form a well-defined structure, and some proteins are entirely disordered[11]. Understanding the functional mechanisms of these systems thus requires detailed knowledge of how molecules can change their shapes or conformations. Key questions are: which interactions are involved, and how are they coupled? Which sequences of events lead from one conformation to another? How heterogeneous are these conformational ensembles? What are the timescales on which these conformational dynamics occur? How do dynamics relate to function? And how are they linked to nonequilibrium processes? Elucidating these aspects of biomolecular dynamics is a key challenge in biological physics, and the development of physical methods is at the heart of progress in this field.

The development of single-molecule spectroscopy in the condensed phase in the 1990s[12,13] soon enabled its application to biomolecular systems[14]. The fundamental ability to avoid signal averaging over large ensembles of molecules provided the opportunity of resolving structural and dynamic heterogeneity and addressing the properties of molecules within complex environments. The resulting close relation to the concepts of statistical physics triggered extensive synergies among experiment, theory and simulations in this field of single-molecule biophysics[15]. One particularly successful single-molecule technique is based on the distance-dependent energy transfer between two suitably chosen fluorophores that are covalently attached to the biomolecule of interest[16]. Overlap between their emission and absorption spectra leads to the resonant and radiationless transfer of electronic excitation energy from the donor to the acceptor fluorophore (Box 1). The $1/r^6$ distance dependence of the rate of energy transfer makes the process a sensitive 'spectroscopic ruler'[17] on the nanometre-length scale, ideal for probing changes and fluctuations in the structures of biomolecules. The theoretical framework that is now used was completed by Theodor Förster in the 1940s[18], so the process is commonly referred to as Förster resonance energy transfer or FRET. Experimental measurements of FRET on biomolecular systems were pioneered in the 1950s to 1970s[17], and the first single-molecule FRET experiments were demonstrated in 1996 (ref. 16), followed by a wave of developments and applications to biomolecular systems[19,20].

Single-molecule spectroscopy has since become an important technique for obtaining information on the structure and dynamics of biomolecules, often in close integration with other methods[20–23]. Many of the challenges in applying the technique are in the chemistry and biology required (i) to prepare and specifically label the molecules of interest[24,25], (ii) to enhance the photophysical and photochemical properties of fluorophores[26,27] and (iii) to perform the measurements in the context of entire cells or organisms[28]. In this Review, however, we will focus on the advances in single-molecule FRET that have been enabled primarily by developments from the physics side, including some of the most important current challenges, and future directions that we consider particularly promising.

Nanoscale dynamics across 12 orders of magnitude in time

Biomolecular dynamics occur across a vast range of timescales, from the femtosecond vibrations of individual covalent bonds to the lifetime of an organism, corresponding to 24 orders of magnitude in time. Covering this considerable range inevitably requires multiple methods, many of which focus on a relatively narrow window in time. Part of the versatility of single-molecule FRET is that it has provided access to dynamics over a large range, from nanoseconds to days[20,29,30]. Before we go into the most recent developments in the field, we will briefly summarize the current state of the art, especially the timescales that are currently accessible, illustrated with examples and the corresponding techniques in Fig. 1.

The detection method is a key factor defining the time resolution of the measurement. Two types of detectors are predominantly used for recording the fluorescence signal from single molecules[31,32]: highly sensitive electron-multiplying charge-coupled devices or complementary metal-oxide-semiconductor cameras, often in combination with total internal reflection microscopy; and single-photon avalanche diodes (SPADs), usually in combination with confocal detection. The advantage of camera-based imaging is that many molecules can be observed simultaneously, but they need to be anchored to the surface

Box 1 | History and principle of Förster resonance energy transfer

Arguably, the first observation of non-radiative resonance energy transfer dates back to Heinrich Hertz: producing oscillating fields with a dipole antenna, Hertz observed sparks across a gap in a nearby resonant receiver. In the 1920s, Cario and Franck[226] performed pioneering measurements of energy transfer between atoms in mixtures of mercury and thallium vapour. They observed the emission spectrum of thallium while illuminating the vapour mixture at a wavelength where only mercury absorbs. The results can be interpreted in terms of the rate of energy transfer, k_T, between a donor (mercury) and an acceptor (thallium), and the spontaneous decay rate of the donor, k_D, owing to radiative and non-radiative relaxation modes in the absence of the acceptor. The probability, or efficiency, of energy transfer can then be expressed as:

$$E = \frac{k_T}{k_D + k_T}.$$

The quantitative use of E requires us to compute k_T, the rate at which the combined state of donor and acceptor fluorophores, D and A, changes from $|D^* A\rangle$ to $|D\, A^*\rangle$, in which * indicates the excited state. The dipole–dipole interaction between the two fluorophores separated by the distance vector $\mathbf{r}$, with dipole moments $\boldsymbol{\mu}_D$ and $\boldsymbol{\mu}_A$, is described by the energy term $V_{DA}=1/(4\pi\varepsilon_0\varepsilon_r)[(\boldsymbol{\mu}_D \cdot \boldsymbol{\mu}_A)/r^3 - (\boldsymbol{\mu}_D \cdot \mathbf{r})(\boldsymbol{\mu}_A \cdot \mathbf{r})/r^5]$. First attempts to describe the phenomenon quantum mechanically were made by Kallmann and London[227], as well as by Perrin[228], but they used a formalism appropriate only for coherent and reversible transfer, which predicted a $1/r^3$ dependence that was not in agreement with experiments on the concentration dependence of fluorescence depolarization.

A complete description of Förster resonance energy transfer requires quantum electrodynamics[229], but sufficiently accurate results can be obtained with a semiclassical approach using perturbation theory in the weak coupling regime[230]. The key steps towards the explanation of the phenomenon were made in the 1940s by Oppenheimer[231] and Förster to explain photosynthesis. Oppenheimer, inspired by the analogy with nuclear decay via internal conversion, correctly derived the transfer rate including incoherent processes but did not publish the results until 1950 (ref. 232). Förster, in his papers of 1946 (ref. 233) and 1948 (ref. 18), accounted for the rapid decoherence[234] of the fluorophores in solution (~10^{14} s^{-1}) relative to the transfer rate (~10^8 s^{-1}) owing to the interactions of the fluorophores with the environment and vibrational motions[235], which effectively produce a continuum of states, as evidenced by the broad emission and absorption spectra of fluorophores in the condensed phase at ambient temperature. As a result, Fermi's golden rule can be used to calculate the transfer rate:

$$k_T = \frac{2\pi}{\hbar} |\langle DA^*|V_{DA}|D^*A\rangle|^2 \rho_{eff},$$

in which $\langle DA^*|V_{DA}|D^*A\rangle$ is the transition matrix element (using the point-dipole approximation) that corresponds to V_{DA}, and ρ_{eff} is the effective density of final states.

The dependence of k_T on the relative orientation between $\boldsymbol{\mu}_D$ and $\boldsymbol{\mu}_A$ can be combined into the parameter κ, resulting in $V_{DA}=1/(4\pi\varepsilon_0 n^2)\,\kappa\,|\boldsymbol{\mu}_D||\boldsymbol{\mu}_A|/r^3$; with the refractive index $n=\sqrt{\varepsilon_r}$ of the medium, k_T becomes

$$k_T = \frac{2\pi}{\hbar}\frac{\kappa^2}{r^6}\frac{|\langle D|\boldsymbol{\mu}_D|D^*\rangle|^2 |\langle A|\boldsymbol{\mu}_A|A^*\rangle|^2}{(4\pi\varepsilon_0)^2 n^4}\rho_{eff}.$$

Of great practical use has been Förster's demonstration[18] that $|\langle D|\boldsymbol{\mu}_D|D^*\rangle|^2|\langle A|\boldsymbol{\mu}_A|A^*\rangle|^2\rho_{eff}$ is proportional to the overlap integral, $J=\int_0^\infty f_D(\lambda)\varepsilon_A(\lambda)\lambda^4 d\lambda$, between the normalized fluorescence emission spectrum of the donor, $f_D(\lambda)$, and the absorption spectrum of the acceptor, $\varepsilon_A(\lambda)$, times Φ_D, the quantum yield of the donor, divided by the donor lifetime in the absence of the acceptor, $\tau_D=1/k_D$. On the basis of these relations, Förster was able to predict the transfer rate, with no free parameters, from the spectra of the fluorophores measured independently. The resulting expression for the transfer efficiency in terms of the Förster radius, $R_0=\sqrt[6]{\frac{9,000\ln(10)}{128\pi^5 N_A}\frac{\kappa^2\Phi_D}{n^4}J}$ (N_A is the Avogadro constant), and the distance between the fluorophores, r, yields

$$E = \frac{1}{1+(r/R_0)^6}.$$

This is the equation most commonly employed to infer distance information from measured values of E. For more details on the history of the theoretical developments, see the excellent review by Clegg[236].

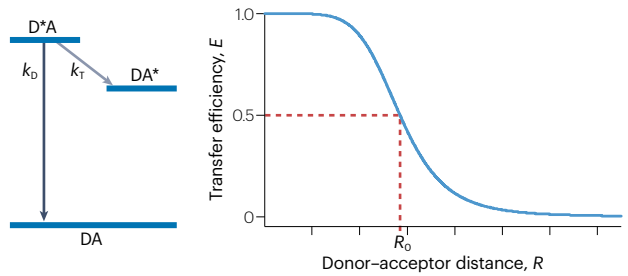

of a microscope cover slide. The time resolution is limited by the frame rate of the camera, typically 10–100 Hz, but with the latest generation of scientific complementary metal-oxide-semiconductor cameras, submillisecond time resolution has been achieved[33,34]. SAPDs provide much higher time resolution, limited essentially by the photon timing jitter[35] of ~50 ps, but because of the point-like detection, individual molecules must be monitored sequentially, either immobilized on a surface or freely diffusing in solution. With this high time resolution, SPADs enable time-correlated single-photon counting and thus access to the complete photon statistics down to the picosecond range[31]. With pulsed laser excitation, time intervals between excitation and emission — and thus fluorescence lifetime decays — can be acquired[36], which are typically in the range of a few nanoseconds. It is these photophysical processes of FRET and the rotational motion of the fluorophores that limit the shortest timescales accessible for probing biomolecular dynamics. The longest timescales over which individual immobilized

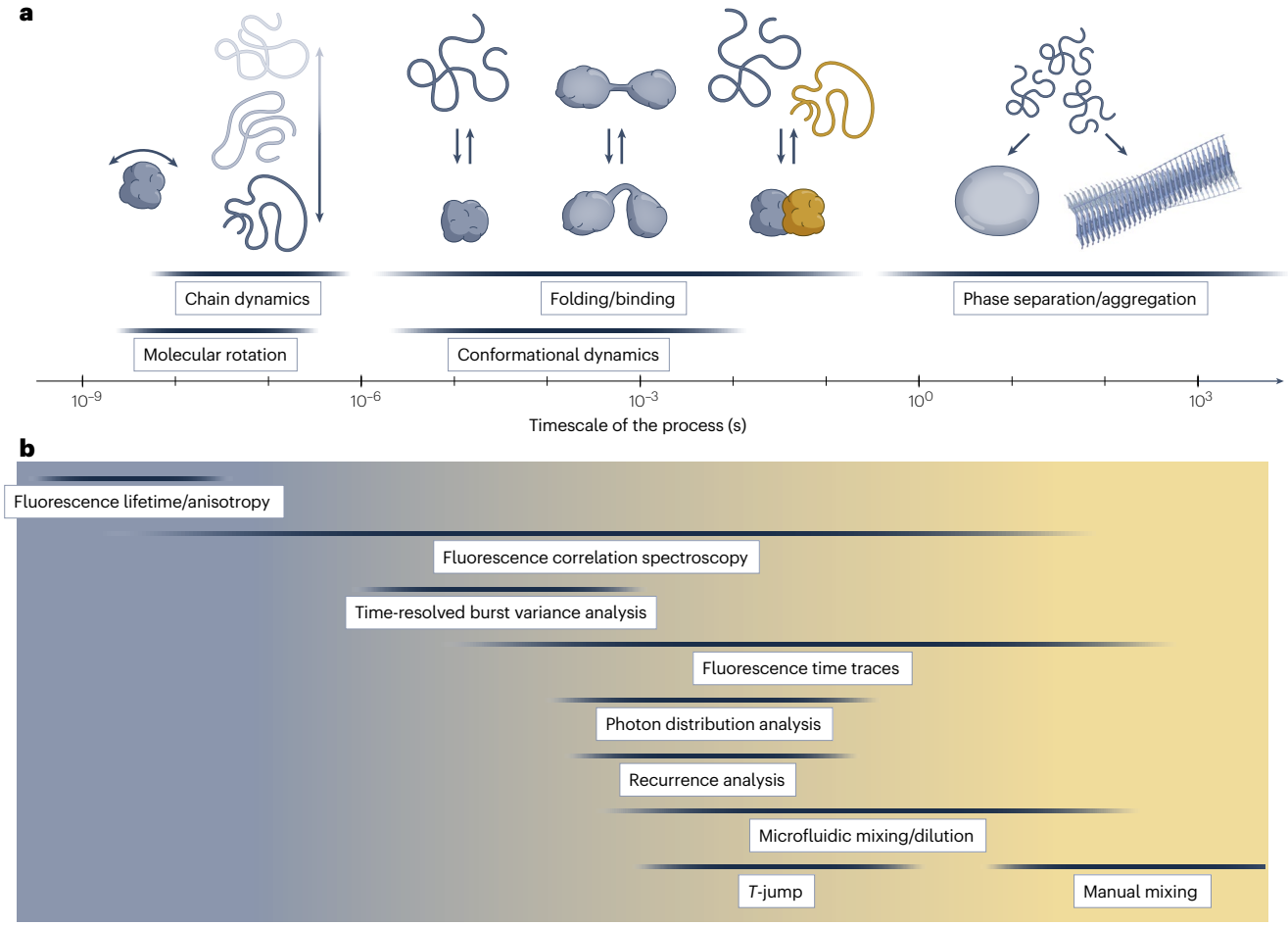

Fig. 1 | Timescales of biomolecular dynamics probed with single-molecule Förster resonance energy transfer. a, Currently available single-molecule Förster resonance energy transfer methods cover more than 15 orders of magnitude in time and allow a wide range of biomolecular dynamics to be investigated. Essentially, all timescales above the lower limit set by the photophysics of the fluorophores can be probed with the available range of experiments and analysis methods. Arrows indicate interconversion between states or configurations. **b**, The approximate time ranges accessible with different techniques[45,210,223–225] (many of which are mentioned in the text) are indicated as horizontal bars.

molecules can be monitored continuously are limited by photobleaching; at sufficiently low excitation rates, observation times of minutes are commonly reached. Although strategies for extending these observation times have been suggested, for example, by replacing the labels continuously[37], longer timescales have mostly been probed on freely diffusing molecules, so that not one individual molecule is monitored as function of time. Instead, the temporal evolution of population distributions is reconstructed from the signal from many individual molecules (see Probing nonequilibrium dynamics)[29].

Accurate single-molecule FRET measurements require at least two detectors, one each for the emission wavelength ranges of the donor and the acceptor dyes. Instruments with four or more detection channels are commonly employed in confocal instruments[38], for instance, to monitor emission from more than two dyes in multicolour FRET, which can provide information on multiple distances simultaneously[39,40]; to separate photons by polarization, which affords important information on the rotational mobility of the fluorophores and thus the validity of rapid averaging over donor–acceptor orientations that greatly simplifies the analysis[38,41]; or to eliminate detector dead times and artefacts from breakdown flashes and afterpulsing[42] in rapid correlation analysis[43]. This multiparameter fluorescence detection[38] offers complementary information beyond simple fluorescence intensities from donor and acceptor, including fluorescence lifetimes, polarization, molecular brightness, diffusivity and so forth, as described in many detailed reviews on the topic[20,38,44–46]. One important challenge, and a focus of this Review, has been to probe rapid dynamics with FRET, in the time range covering much of the interesting molecular dynamics.

Resolving rapid dynamics

To conceptualize biomolecular dynamics, let us consider a process such as the conformational change of a protein, its folding or a binding reaction. A complete description of this process would require knowledge of the detailed forces and motion of all atoms of the system, including the solvent, as a function of time. However, experiments can only provide information on a small fraction of all degrees of freedom. It is thus instructive to choose a simplified description, for instance, in terms of diffusion on a free-energy surface[15,47]. The free energy is then represented as a function of a small number of reaction coordinates

that reflect the process of interest, and the dynamics are approximated in terms of diffusive motion on this free-energy surface. Chemical kinetics is concerned with the interconversion rates between metastable states, which are related to the dwell times (or waiting times) in the minima of the free-energy surface. A physically more complete picture of the dynamics additionally includes an explicit description of the relaxation within the individual free-energy minima, and of the actual process of crossing the free-energy barrier when a transition occurs, the transition paths[15,48,49] (Box 2 explains these aspects in detail). Whenever these processes lead to changes in intra- or inter-molecular distances, they can in principle be probed with single-molecule FRET experiments. As inter-dye distance changes result in anticorrelated emission probabilities of donor and acceptor, distance dynamics can be reliably distinguished from other sources of emission fluctuations[45], such as quenching by nucleotides and aromatic amino acids, or triplet blinking[26].

A powerful way of analysing photon time series from single-molecule FRET experiments is the use of hidden Markov models[50–53] (see Box 3 and the section on Advances in data analysis and modelling), which have enabled dynamics to be resolved down to the microsecond range[30,48]. Another widely employed approach for measuring distance dynamics is fluorescence correlation spectroscopy[54–56] (FCS), a versatile and virtually model-free way of analysing photon statistics across a wide range of timescales. By combining FCS with single-molecule FRET and fluorescence lifetime information, the dynamics of individual subpopulations of molecules can be resolved[45,56–58]. On the basis of the known distance dependence of FRET (Box 1), correlation functions can be quantitatively related to distance dynamics, using either analytical models or simulations. An example in which such measurements have been important to probe very rapid molecular motion is the chain dynamics of unfolded and intrinsically disordered proteins[45] (Box 2). Reconfiguration times — the relaxation times of end-to-end distance correlation functions — for chain lengths of about a hundred residues range from tens to hundreds of nanoseconds[45,59]. Some disordered proteins even remain disordered when bound to their interactions partners[60,61], which can lead to a moderate[62] or pronounced[63] slowdown of their dynamics.

The fastest molecular motions we can detect with single-molecule FRET combined with correlation analysis are limited by photophysics[64]. This limit arises because the fluorescence fluctuations in the range of the excited-state lifetimes of the dyes are dominated by the electronic transitions between ground and excited states, which lead to the photon antibunching characteristic of individual quantum systems[65] (Box 2 and Fig. 2c). As a result, measuring distance dynamics faster than ~10 ns has been challenging, because the components of the correlation functions related to distance dynamics are difficult to separate from photon antibunching. An additional factor essential for the time resolution is the photon detection rate from individual molecules. Values above $10^5\,s^{-1}$ are often difficult to achieve because of limitations in detection efficiency and rapid photobleaching at high excitation rates, so the probability of observing photons separated by submicrosecond time intervals is low. Correspondingly, accumulating sufficient photon statistics for quantifying submicrosecond distance dynamics can require very long measurements of 10 h or more[45], and dynamics in the low nanosecond range have essentially been impossible to probe. Examples of dynamics expected in this range are the chain reconfiguration of short polypeptides or oligonucleotides; higher relaxation modes of longer chains; loop regions in folded proteins; or the actual motion of fluorophores attached to a biomolecule.

Similarly, for experiments aimed at resolving transition paths between metastable conformational states of molecules (Box 2), the relatively low fluorescence emission rates[48] have limited the time resolution of single-molecule experiments. Transition paths are of great interest, because they contain much of the key information on the molecular mechanisms underlying conformational changes or folding processes[66]. However, the experimental observation of transition paths is challenging, for two main reasons. First, for activated processes, these events are rare, because the molecule spends most of its time in the free-energy minima and only rarely jumps across the barrier, so most of the signal collected reports on the relaxation dynamics during the waiting times within the minima. Second, transition paths are short — often in the microsecond range[48] — so that very high photon rates are required even to estimate just the duration of the transition. In practice, this means that the transitions from many single-molecule FRET recordings, with only a few photons per transition, have had to be combined in a maximum-likelihood analysis[67] to obtain transition path times. Resolving individual transition paths on the microsecond timescale with, say, 100 photons during the transition would require the photon detection rates to be enhanced by about two orders of magnitude.

Plasmonic enhancement of fluorescence for FRET

Arguably, the most promising strategy towards single-molecule FRET experiments with higher time resolution is the plasmonic enhancement of fluorescence in the near field of metal nanostructures (Fig. 2). For an emitter near a metal nanoparticle, two contributions are important to consider[68]. The first is the Purcell effect[69] of the environment on the local density of optical states[70], which changes the emission rate, as described by Fermi's golden rule[71]: if an emitter is placed near a metal nanoparticle, coupling of the external electromagnetic field with the surface plasmon modes of the conduction electrons provides additional radiative decay channels for the emitter that reduce its fluorescence lifetime[72,73] — a process analogous to FRET to an acceptor fluorophore that can itself be used for sensitive distance measurements[74–77]. The second contribution is that the excitation of localized surface plasmon resonances in nanoparticles by incident light can lead to pronounced field enhancements close to the surface of the particle or nanostructure, resulting in the concentration of electromagnetic fields into subdiffraction volumes[78]. The electric field in these small volumes can be intense, leading to the formation of plasmonic hotspots with field enhancements by orders of magnitude. Placing a fluorophore into such a hotspot can thus greatly increase the efficiency of excitation.

The influence of plasmonic enhancement on fluorescence has long been recognized[79], and many geometries of nanocavities and nanoantennas have been proposed to concentrate the local field most effectively[68,80]. One challenge is that the geometric effects on the fluorophore are highly dependent on its distance from the nanoparticle surface, and optimal enhancement with constant efficiency requires precise positioning of the molecule in the hotspot. An elegant solution to this problem is the use of DNA origami for the self-assembly of scaffolds that enable the positioning of individual molecules relative to plasmonic nanoparticles with nanometre precision[81–83] (Fig. 2a). On the basis of such self-assembled nanoantennas, enhancement of individual fluorophores by more than two orders of magnitude have been achieved. The technique also shows great promise in terms of monitoring distance dynamics with much higher time resolution when combined with single-molecule FRET on immobilized molecules[82,84].

Box 2 | Dissecting biomolecular dynamics with single-molecule Förster resonance energy transfer

We use the term 'dynamics' to describe all molecular motion in the system of interest. Experiments, however, only provide limited information on a few degrees of freedom, so how can we describe biomolecular dynamics based on this information with simple quantitative models?

One approach, originally developed for chemical reactions, and widely used for describing biomolecular dynamics, is to employ kinetics as described by the reaction rate or master equations. This approximation is suitable for processes characterized by a few metastable states separated by high barriers, which results in a separation of timescales between the rapid conformational dynamics within the metastable states on the one hand and the much slower rates of crossing the barriers on the other. In this description, the dynamics within states are ignored, and the barrier crossing process is assumed to be instantaneous. The underlying cooperative transitions thus lead to long waiting times in the minima that are exponentially distributed. These dwell time distributions and the corresponding rate coefficients can be inferred from single-molecule recordings[51,146] (see the figure and Box 3).

There are, however, many processes that do not involve clearly separable states, for instance, the fluctuations within a metastable state, such as the conformational ensemble of an unfolded protein. A simple description of such overdamped dynamics involves the timescale of these fluctuations and their amplitude about a mean value, which can be represented in terms of diffusion in a potential of mean force (see the figure) with a shape inferred from experimental data or simulations. Even rapid conformational fluctuations down to the nanosecond range can be resolved with fluorescence correlation spectroscopy[45,237] (see the figure).

With these two concepts, we can describe both the fluctuations within states and the rates of the rare transitions between them, but what about the actual barrier crossing process across the transition state? In contrast to simple kinetics, in which these transitions are treated as instantaneous jumps, their actual duration is of course finite. In fact, these transition paths are often the most interesting part of the process, because this is when the cooperative changes in conformation that define the detailed molecular mechanism actually occur[66]. Transition paths are challenging to probe, as they are short, rare events, and the times at which they occur are stochastically distributed. However, single-molecule FRET provides the opportunity to resolve transition paths[48] (see the figure).

The combination of rate-based kinetics, conformational fluctuations and transition paths allows many aspects of biomolecular dynamics to be described quantitatively. For dynamics on much

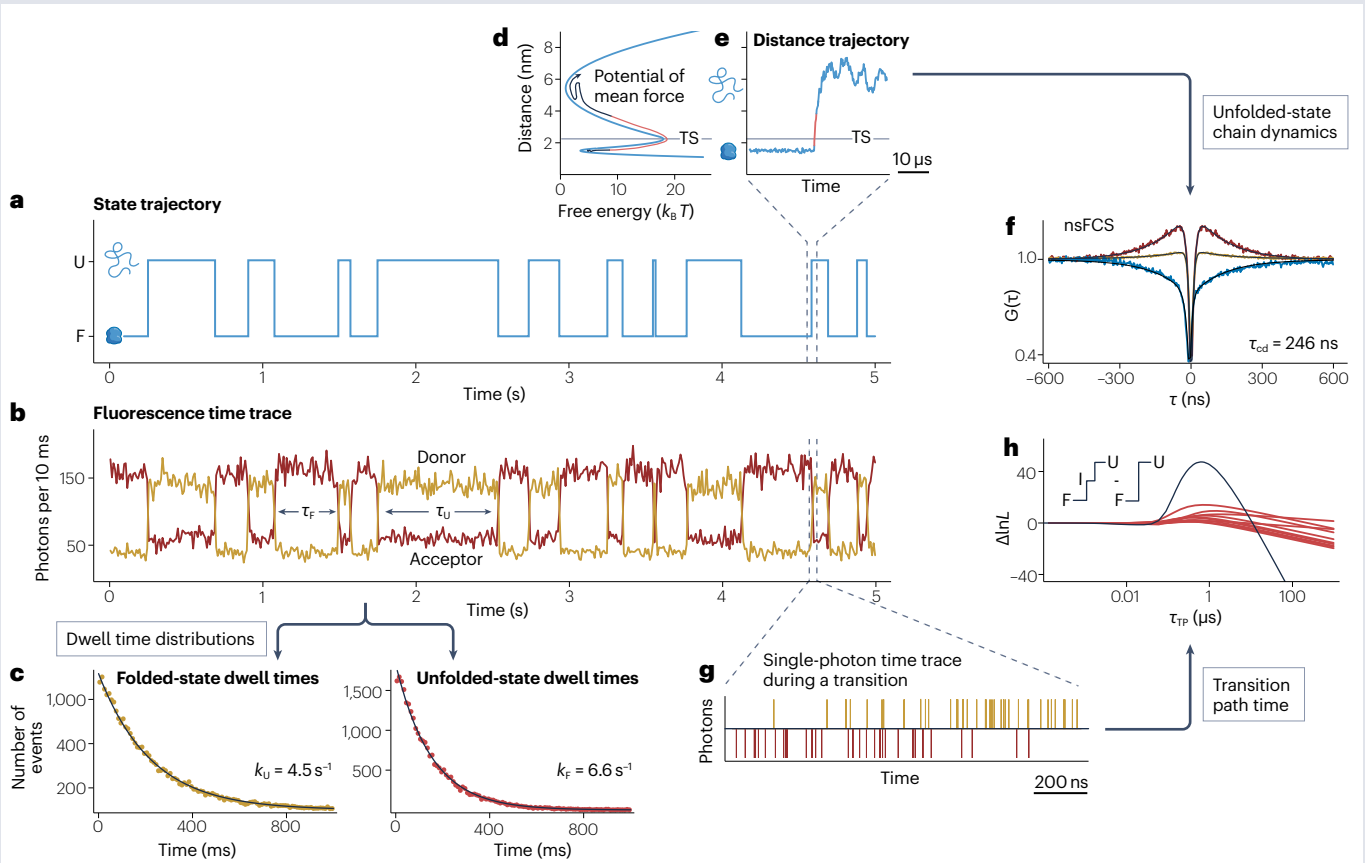

(continued from previous page)
shorter timescales, it may be important to additionally consider contributions from inertial motion or quantum effects.

The figure illustrates these aspects of dynamics for the example of protein folding, where the equilibrium between the folded (F) and unfolded states (U) of a protein is probed with single-molecule FRET. A two-state trajectory (part **a**) and the corresponding photon emission from donor (green) and acceptor (red) (part **b**), with the resulting exponential dwell time distributions identified with the Viterbi algorithm[238] (part **c**). A 1D free-energy surface of the process (TS, transition state) (part **d**), with the diffusive dynamics on this potential near a transition (orange segment: transition path) (part **e**). **f**, Rapid distance dynamics in the unfolded state can be probed with nanosecond FCS (nsFCS; donor and acceptor autocorrelations: green and red, respectively; cross-correlation: blue; fits: black lines). τ_{cd}, the mean correlation time of the chain dynamics, is obtained from fitting the curves. **g**, Time-resolved recording of photon emission during a transition (example using 30 MHz average count rate, a regime that is starting to come into reach[84]) can be used for a likelihood-based analysis of transition path times (part **h**)[67]. $\Delta \ln L$ is the difference between the log-likelihoods for a model that assumes a virtual intermediate (I) mimicking a transition state of finite lifetime and for an instantaneous transition, yielding in this example a most likely transition path time, τ_{TP}, of ~1 µs (orange: results from 10 individual photon time traces; black: sum). The data shown were simulated based on a two-state Markov model (parts **a** and **b**), or in terms of diffusion on a free-energy surface by discretizing the potential and using a discrete random walk with microscopic rate coefficients (**e**–**g**). Note that higher photon rates were used for simulating part **g** than for part **b**.

In a complementary approach, nanoapertures in a thin metal film deposited on glass have been employed as zero-mode waveguides (ZMWs)[85]. As the name indicates, these waveguides provide no modes for the propagation of light owing to their subwavelength size[86]. Instead, incident light forms an evanescent field with a steep amplitude decay in the tens to hundreds of nanometre range (Fig. 2b). The combination of the evanescent field depth with the small diameter of the aperture of ~100 nm yields effective observation volumes of attolitres, orders of magnitude smaller than diffraction-limited confocal volumes[85,87]. The resulting ability to perform single-molecule measurements at much higher concentrations of fluorescent samples has led to important technological developments, such as high-throughput DNA sequencing in large arrays of ZMWs in which individual DNA polymerase molecules are immobilized[88].

ZMWs have also been employed for the enhancement of single-molecule fluorescence[87,89]. The application to single-molecule FRET, however, had been questioned because of the complex influence of the extreme field confinement on the decay rates and the quantum yields of the donor and acceptor and the transfer rates between them. In addition, the presence of field components in all spatial directions in the ZMW (Fig. 2b) is expected to lead to deviations from the canonical distance dependence of FRET[90]. Recent systematic results as a function of ZMW diameter demonstrate the feasibility of single-molecule FRET measurements on freely diffusing[90–92] and immobilized[93] molecules; the plasmonic enhancement increases the fluorescence detection rate by up to an order of magnitude and extends the accessible distance range by several nanometres. Although the accuracy of FRET measurements for obtaining absolute distance information may be compromised, the deviations from the r^6 dependence (Box 1) seem to be moderate for donor–acceptor distances near the Förster radius[90,94]. However, assessing the quantitative implications of such effects will be an important aspect of future research.

The enhancement of fluorescence emission rates in ZMWs is expected to be particularly useful for improving measurements of very rapid dynamics or short events, because the probability of recording photons at high rates is increased. A recent example is the measurement of nanosecond FCS (nsFCS) on freely diffusing molecules in ZMWs, in which an increase in the signal-to-noise ratio by almost an order of magnitude reduced data acquisition times from ~10 h to tens of minutes[94] (Fig. 2c). nsFCS measurements also benefit from the reduced fluorescence lifetimes owing to the increased local density of optical states in the ZMWs, which improves the separation of timescales between photon antibunching and rapid distance dynamics. This effect has enabled measurements of distance dynamics by FRET down to a few nanoseconds[94], a regime that has previously been difficult to access.

Plasmonic enhancement is also a promising strategy for single-molecule FRET measurements with high time resolution on immobilized molecules, for instance, with molecules placed at optimal positions relative to nanoantennas using DNA origami[82]. An application of great current interest is the measurement of transition path times[15,48,49,95] (Box 2), whose durations in the microsecond range have been measured with single-molecule FRET for some protein folding[48] and binding reactions[96–98]. For resolving transition paths in more detail, however, an enhancement of photon rates by at least one or two orders of magnitude will be required; nanoantennas provide a promising strategy towards this goal[84] (Fig. 2a).

Nanophotonics thus offer great opportunities for advances in probing rapid biomolecular processes, but many open questions remain. One challenge is a more quantitative understanding of the complex combination of contributions that influence single-molecule FRET near metal nanostructures, including (i) the Purcell effect and its influence on fluorescence lifetimes and quantum yields; (ii) the strong field enhancement near the localized potential gradients at the edges of nanoapertures (Fig. 2b); (iii) changes in the fluorescence collection efficiency owing to the altered emission patterns of dipoles near nanostructres[68,87]; (iv) the modulation of the dependence of FRET on the relative orientation of donor and acceptor owing to electric field components along all three directions of space[99]; (v) the averaging over the heterogeneous diffusive paths in and out of the nanoaperture and (vi) nonlinear photophysical effects. The example of ZMWs illustrates that even very simple geometries can be powerful, but advanced geometries provide many further opportunities[68,80,100]. Another challenge is that the potentially very high photon rates may require new detector technology with short dead times, such as single-photon detectors based on superconducting nanowires[101].

Perturbation techniques for nonequilibrium dynamics

In most ensemble measurements, information on dynamics is obtained by synchronizing the molecular ensemble by means of a perturbation

Box 3 | Single-molecule fluorescence time traces analysed as continuous-time hidden Markov processes

Time traces of fluorescence photons collected from single molecules are often analysed using hidden Markov models. The underlying idea is that the observed molecule is a dynamic system visiting different states that represent local minima in the corresponding free-energy landscape (Box 2). For example, a change in conformation or the binding to a target corresponds to the spontaneous crossing of an energy barrier between corresponding minima. Neglecting the dynamics within the states and the details of barrier crossing (Box 2), we can describe the dynamics as stochastic jumps between states with exponential distributions of the times between them. Such a continuous-time Markov process can be represented by a kinetic scheme of the kind shown in the enclosed illustration. Using the kinetic rate matrix $\mathbf{K}$, we can describe the stochastic time evolution of the system by $\mathbf{p}(t) = e^{\mathbf{K}t}\mathbf{p}(0)$, in which $\mathbf{p}(t)$ is the probability vector for being in states S_1, S_2, S_3 at time t.

The goal of the analysis is to find the most appropriate kinetic model, $\mathbf{K}$, that describes the experimental data. The time trace can be formalized as a sequence of observations, $\mathbf{z} = (\tau_1, c_1, \tau_2, c_2, \ldots, \tau_T, c_T)$. Here, τ_k are the interphoton times, and c_k symbolizes the 'colour' of the kth photon detected; for FRET measurements, c_k is either D or A. The system is a hidden Markov model because a single observed photon does not unambiguously reveal which state the molecule is in. Instead, we only know the probabilities of detecting a donor or acceptor photon and of not detecting any photon for a given time interval while the molecule is in a certain state. For example, we might know the mean donor and acceptor photon rates; assuming exponentially distributed interphoton times for each state, one can then calculate the probability $P(\mathbf{z}|\mathbf{K})$ of the time trace $\mathbf{z}$, given a hypothetical rate matrix $\mathbf{K}$. This calculation turns out to be extremely useful, because Bayes' theorem relates this probability to the more interesting posterior probability, $P(\mathbf{K}|\mathbf{z})$, for a hypothetical $\mathbf{K}$ given the evidence $\mathbf{z}$, by $P(\mathbf{K}|\mathbf{z}) = P(\mathbf{z}|\mathbf{K}) \cdot P(\mathbf{K})/P(\mathbf{z})$. In the theory of Bayesian inference, $P(\mathbf{z}|\mathbf{K})$ is called the likelihood (here now viewed as a function of $\mathbf{K}$ instead of $\mathbf{z}$), $P(\mathbf{K})$ is the prior probability, and $P(\mathbf{z})$ is the marginal likelihood. Maximum-likelihood estimation is a powerful method for finding the most probable $\mathbf{K}$ of the posterior probability distribution $P(\mathbf{K}|\mathbf{z})$ by maximizing the computable likelihood $P(\mathbf{z}|\mathbf{K})$ with respect to the model parameters (assuming $P(\mathbf{K})$=const).

Gopich and Szabo[146] showed that the likelihood for the time trace of donor and acceptor photons can be calculated elegantly and without the need for time binning from

$$P(\mathbf{z}|\mathbf{K}) = \mathbf{1}^T \left(\prod_{k=1}^{T} \mathbf{N}_{c_k} e^{(\mathbf{K}-\mathbf{N})\tau_k} \right) \mathbf{p}_{\mathrm{eq}},$$

as illustrated for the time trace in the figure. Simply put, the term $e^{(\mathbf{K}-\mathbf{N})\tau_k}$ describes how the state probabilities evolve during the intervals τ_k, in which no photons are detected, and the matrices $\mathbf{N}_{c_k}$ reflect the probability that in the next moment a photon of colour c_k is detected. The equation is very powerful for the photon-by-photon interpretation of photon time traces in terms of kinetic models. For binned time traces, such as those recorded in total internal reflection microscopy, the more familiar techniques for discrete-time hidden Markov models must be used[50–52], which typically make the simplifying assumption that emissions and transitions occur only at the boundaries (or midpoints) of the time bins.

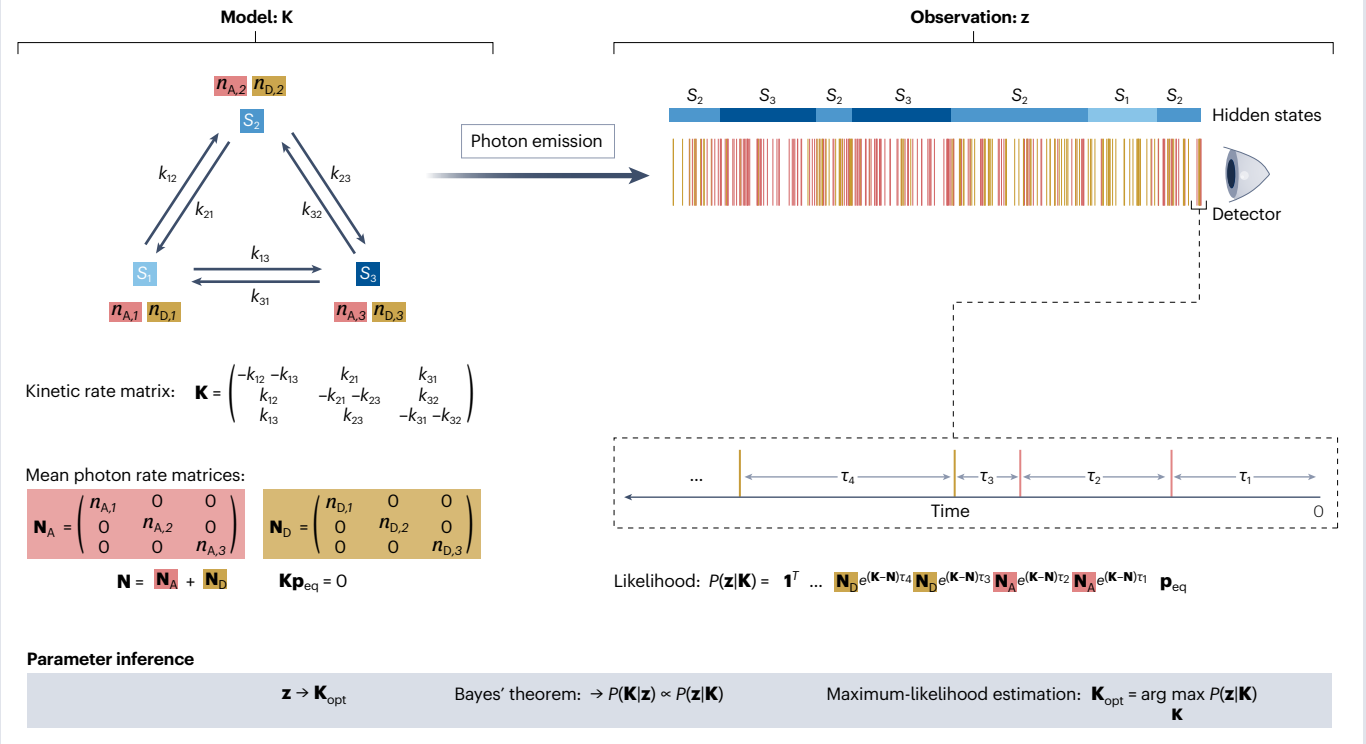

and monitoring its relaxation to equilibrium, for example, by laser-induced temperature jumps or rapid mixing[102]. A notable strength of single-molecule measurements is that dynamics can often be quantified from equilibrium or steady-state experiments[15] (Box 2). However, even in single-molecule experiments, it remains indispensable for many questions to apply perturbations for probing nonequilibrium

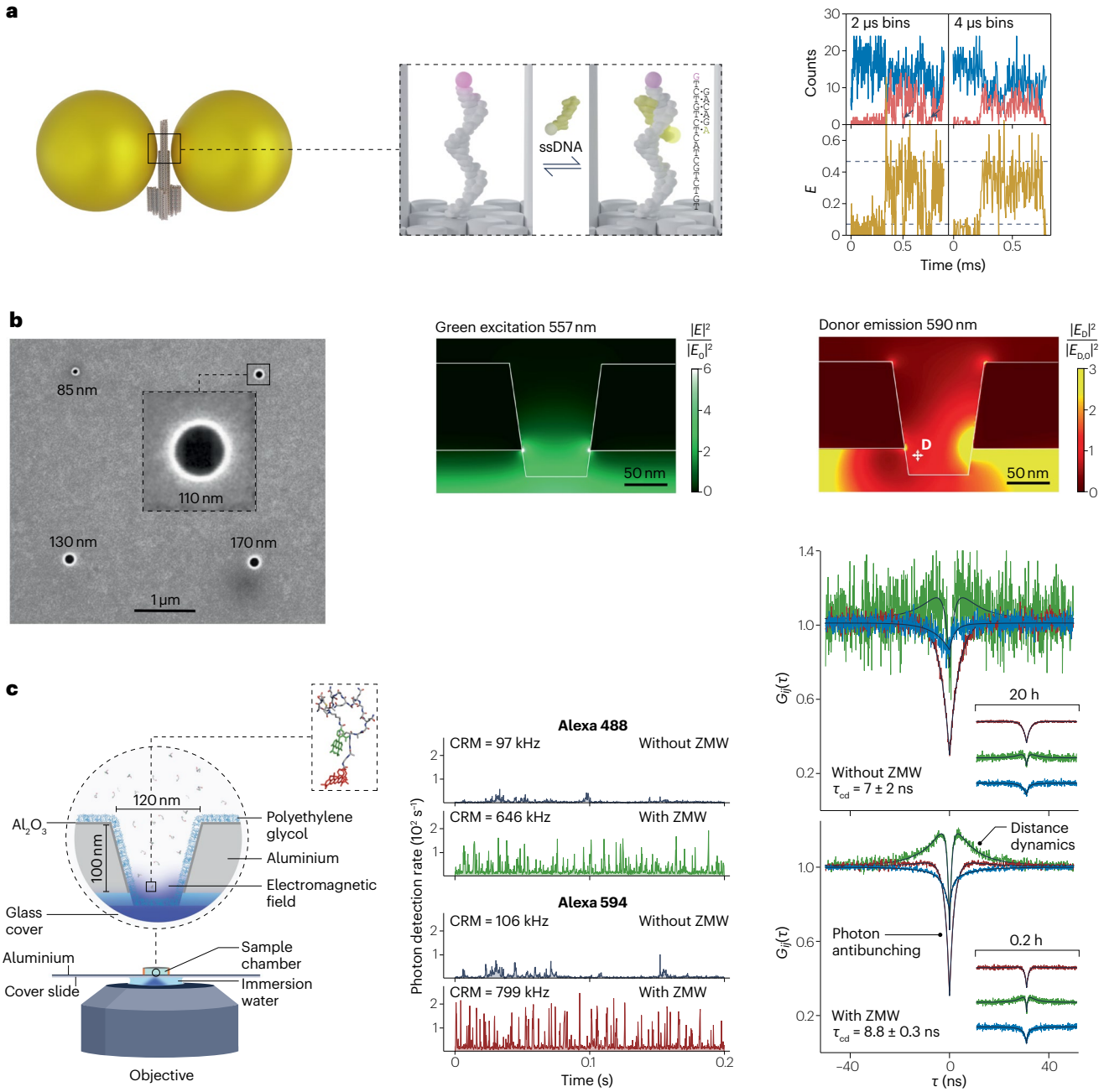

Fig. 2 | Nanophotonic enhancement of fluorescence for single-molecule spectroscopy. a, Illustration of a DNA origami nanoantenna with 100 nm gold nanoparticles that enable positioning of a biomolecule for fluorescence enhancement. Zoom: acceptor-labelled single-stranded DNA (ssDNA) hybridizes with a donor-labelled docking site. Fluorescence time traces show enhanced donor (blue) and acceptor (red) fluorescence during a binding event with high count rates (from ref. 84). **b**, Scanning electron microscope image of aluminium ZMWs with different diameters, and numerical calculations of the electric field intensity enhancement inside a 110-nm ZMW for 557-nm donor excitation (green) and 590-nm donor dipole radiation (red/yellow; from ref. 90). **c**, Left: schematic of confocal measurements of a peptide labelled with Alexa 488 and 594 in a ZMW. Right: fluorescence traces of donor and acceptor emission without (grey) and with ZMW (green, red) illustrate the fluorescence enhancement of molecules diffusing through the nanoapertures. The average count rates per molecule (CRMs) are indicated. Overlay of donor (green) and acceptor (red) fluorescence autocorrelations and donor–acceptor cross-correlations (blue) from measurements of the peptide without ZMW (top) and with ZMW (bottom) after 7 h of data acquisition (inset in part **a** after 20 h and in part **b** after 0.2 h of data acquisition) illustrates the gain in signal to noise (from ref. 94). ZMW, zero-mode waveguide.

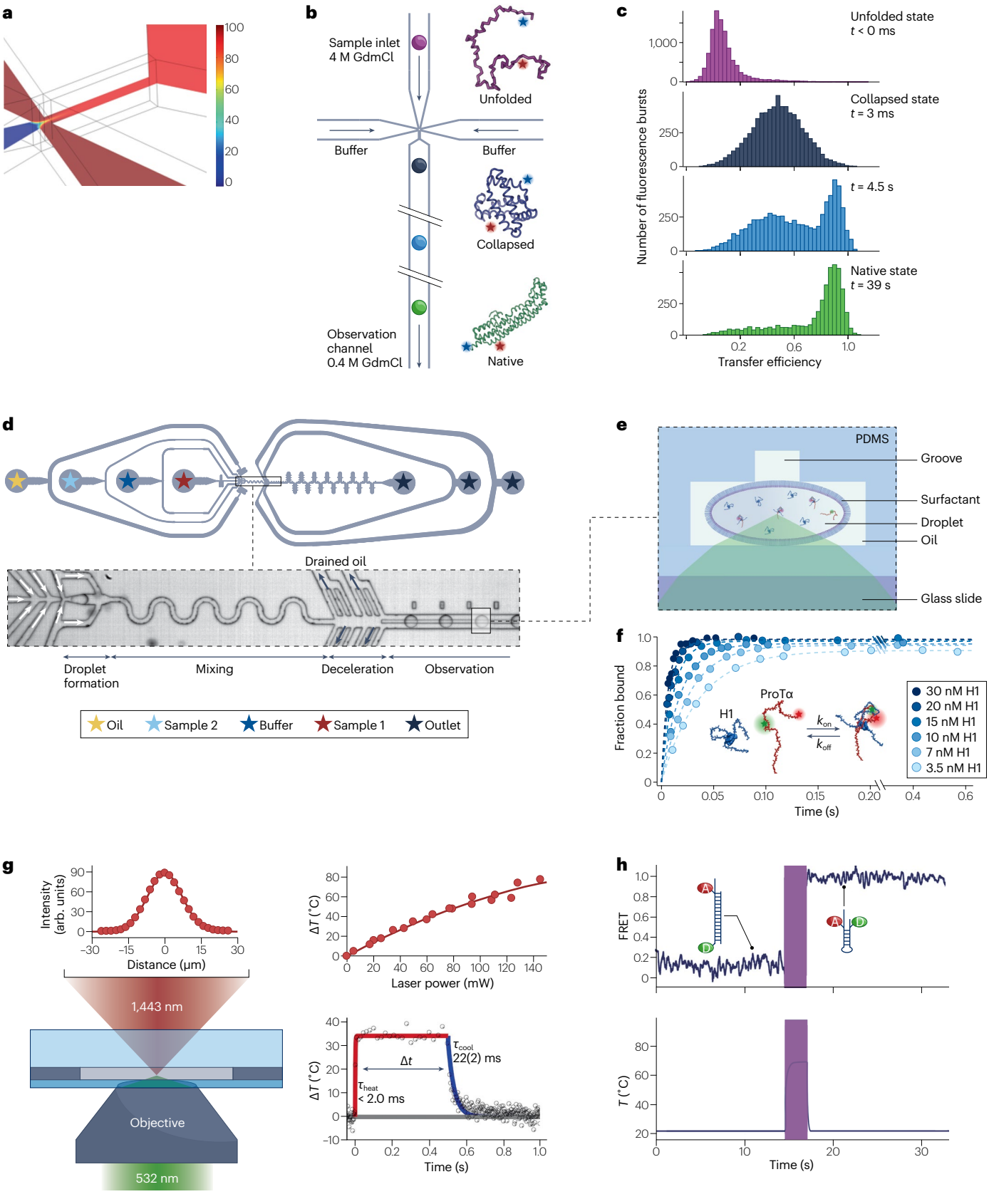
a
100
80
60
40
20
0
b
Sample inlet
4 M GdmCl
Unfolded
Buffer
Buffer
Collapsed
Observation
channel
0.4 M GdmCl
Native
c
Unfolded state
t < 0 ms
Collapsed state
t = 3 ms
t = 4.5 s
Native state
t = 39 s
Number of fluorescence bursts
1,000
250
0.2
0.6
1.0
Transfer efficiency
d
Drained oil
Droplet
formation
Mixing
Deceleration
Observation
Oil
Sample 2
Buffer
Sample 1
Outlet
e
PDMS
Groove
Surfactant
Droplet
Oil
Glass slide
f
Fraction bound
ProTα
H1
k_{on}
k_{off}
30 nM H1
20 nM H1
15 nM H1
10 nM H1
7 nM H1
3.5 nM H1
Time (s)
g
Intensity
(arb. units)
Distance (μm)
1,443 nm
Objective
532 nm
ΔT (°C)
Laser power (mW)
τ_{cool}
22(2) ms
Δt
τ_{heat}
< 2.0 ms
Time (s)
h
FRET
A
D
T (°C)
Time (s)

Fig. 3 | Nonequilibrium single-molecule dynamics. a, A concentration profile from 3D finite-element calculations of the millisecond mixing process in a laminar-flow mixer based on diffusion[108]. The relative concentration of molecules entering from the side channels is colour-coded from 0% to 100%. **b**, Illustration of microfluidic mixing and single-molecule Förster resonance energy transfer (FRET) measurements along the observation channel. Upon rapid dilution of the unfolded protein ClyA with buffer solution, the protein rapidly collapses, followed by slow refolding to the native state[118]. **c**, Examples of transfer efficiency histograms measured at different times in the observation channel. **d**, Schematic of a droplet-based microfluidic mixing device. The zoom-in depicts an optical microscope image with regions indicated corresponding to sample delivery, droplet formation, mixing, deceleration, and droplets moving along the observation channel[124]. **e**, Schematic cross-section of the observation channel, showing a surfactant-stabilized water droplet in oil containing fluorophore-labelled protein molecules (not to scale) passing through the laser focus (excitation beam indicated in green). **f**, Example of millisecond protein association kinetics of the highly charged, disordered proteins ProTα and H1 at different H1 concentrations[124]. **g**, Left: schematic representation of a laser temperature jump apparatus[136]. The infrared (red) and excitation laser (green) foci are aligned coaxially, with the measured radial intensity profile at the focus of the infrared heating laser. Right: the steady-state temperature rise (ΔT) as a function of incident laser power, and the heating and cooling times of IR are experimentally measured. **h**, Laser-induced T-jump allows single-molecule FRET measurements of DNA double helix melting[135]. PDMS, polydimethylsiloxane.

dynamics. Take, for instance, a protein that, at equilibrium, spends most of its time in the folded state; say, on average it unfolds every 10 s but remains in the unfolded state for only a millisecond before it folds again. Satisfying the sampling rate requirements for both states is essentially impossible with current fluorophores: for an excitation rate sufficiently high to enable the reliable detection of the millisecond dwells, photobleaching would occur on a timescale much shorter than 10 s; for an excitation rate low enough for monitoring the 10-s dwell times, the millisecond dwells will largely remain undetected. Even larger differences in the forward and backward reaction rates are not uncommon in biomolecular systems, resulting in processes that are effectively only observable in nonequilibrium measurements. Such experiments typically involve preparing the system in the less stable state, for instance, using solution conditions that favour its population, and then switching to the conditions of interest and monitoring the kinetics of interconversion. Slow kinetics on a timescale of seconds and above can be monitored by manual mixing or with simple flow cells, but for higher time resolution, dedicated instrumentation is required.

A versatile method for resolving rapid nonequilibrium processes in combination with single-molecule FRET is microfluidic mixing[29,103,104]. Most designs used to date are based on hydrodynamic focusing[105,106]. In contrast to turbulent mixing, which is the dominant mechanism at high Reynolds numbers[107], hydrodynamic focusing can be used to form fluid jets with a width of a micrometre or less, a length scale over which mixing is entirely diffusive[106]. An added advantage is that such laminar fluid dynamics at very low Reynolds numbers are amenable to an accurate description in terms of the Navier–Stokes equation[106], which enables precise device design based on finite-element calculations[108,109] (Fig. 3a). Mixing times down to a few microseconds have been achieved[105,110,111]. However, detecting a sufficient number of photons from a single fluorescent molecule to assess transfer efficiencies and distances takes at least hundreds of microseconds at the count rates commonly attained; to enable correspondingly long residence times in the confocal volume, the mixing devices for single-molecule FRET thus typically work in the low millisecond regime and above[108,109,112–115].

The basic idea of continuous-flow microfluidic mixing experiments is to rapidly mix different solutions to trigger the reaction of interest, such as the association of two molecular binding partners or the refolding of a protein. The confocal observation volume is placed at different positions along the observation channel to monitor different times after mixing, from which the kinetics of the process can then be reconstructed (Fig. 3b,c). The upshot is that detailed single-molecule FRET measurements become feasible for states far from equilibrium[108,109,112–115]. An example is the dynamics of compact unfolded states and other conformational intermediates that are hardly populated at equilibrium. By rapidly diluting a solution of a protein unfolded at high concentrations of denaturant, these configurations can be investigated at short times after mixing, before folding to the native state takes place[59,116–118] (Fig. 3b,c). Another example is the formation of transient states in association reactions, such as the intermediate of the intrinsically disordered protein α-synuclein during the binding to detergent micelles[114]. Recent device designs enable dilutions by up to five orders of magnitude within a few milliseconds, which allows low-affinity biomolecular complexes to be probed before they dissociate[119,120], and double-jump mixing devices that combine two consecutive rapid mixing steps separated by an intermediate delay channel[121] for probing multistep reactions.

There are still many opportunities for combining microfluidics with single-molecule spectroscopy. One promising strategy is the use of droplet microfluidics[122], in which rapid mixing is enabled by chaotic advection within aqueous droplets formed in an oil phase moving through a narrow serpentine channel[123]. Yang et al.[124] recently showed that this approach is amenable to single-molecule FRET, with dead times in the range of a few milliseconds (Fig. 3d–f). The droplets represent individual picolitre containers lined with stabilizing surfactants to minimize surface adhesion of biomolecules both to the channel walls and to the oil–water interface. The surfactants enable the investigation of even very delicate proteins whose surface adhesion is too pronounced for laminar-flow microfluidics. Moreover, the position-to-time conversion of measurements along the observation channel is simplified, given the known droplet velocity and the absence of Taylor dispersion — the combined effect of diffusion and shear flow on the dispersion of the molecules along the channels in laminar-flow designs[125,126]. As the droplets do not exchange components with the exterior as they travel through the device, the observation time can be extended to hours or days with long observation channels or storage arrays[127]. Other promising future developments include the combination with advanced detection modalities[127] such as three-colour FRET[119,128,129], temperature control[108,130,131], rapid laser-based triggering techniques or the downstream addition of reagents by picoinjection[132] for monitoring multistep reactions. Integrating ZMWs[133] or other nanophotonic devices with microfluidic mixing may allow us to take advantage of the microsecond mixing times attainable with hydrodynamic focusing[110] and nonequilibrium single-molecule FRET at concentrations up to the micromolar range.

An orthogonal approach for enabling nonequilibrium single-molecule FRET measurements is the use of rapid temperature jumps, for instance, by infrared laser excitation of an overtone of the vibrational OH stretch mode of water[134–136]. By heating a small volume, an increase in solvent temperature on the millisecond timescale has been achieved[135,136] (Fig. 3g–i). This elegant technique has been used to

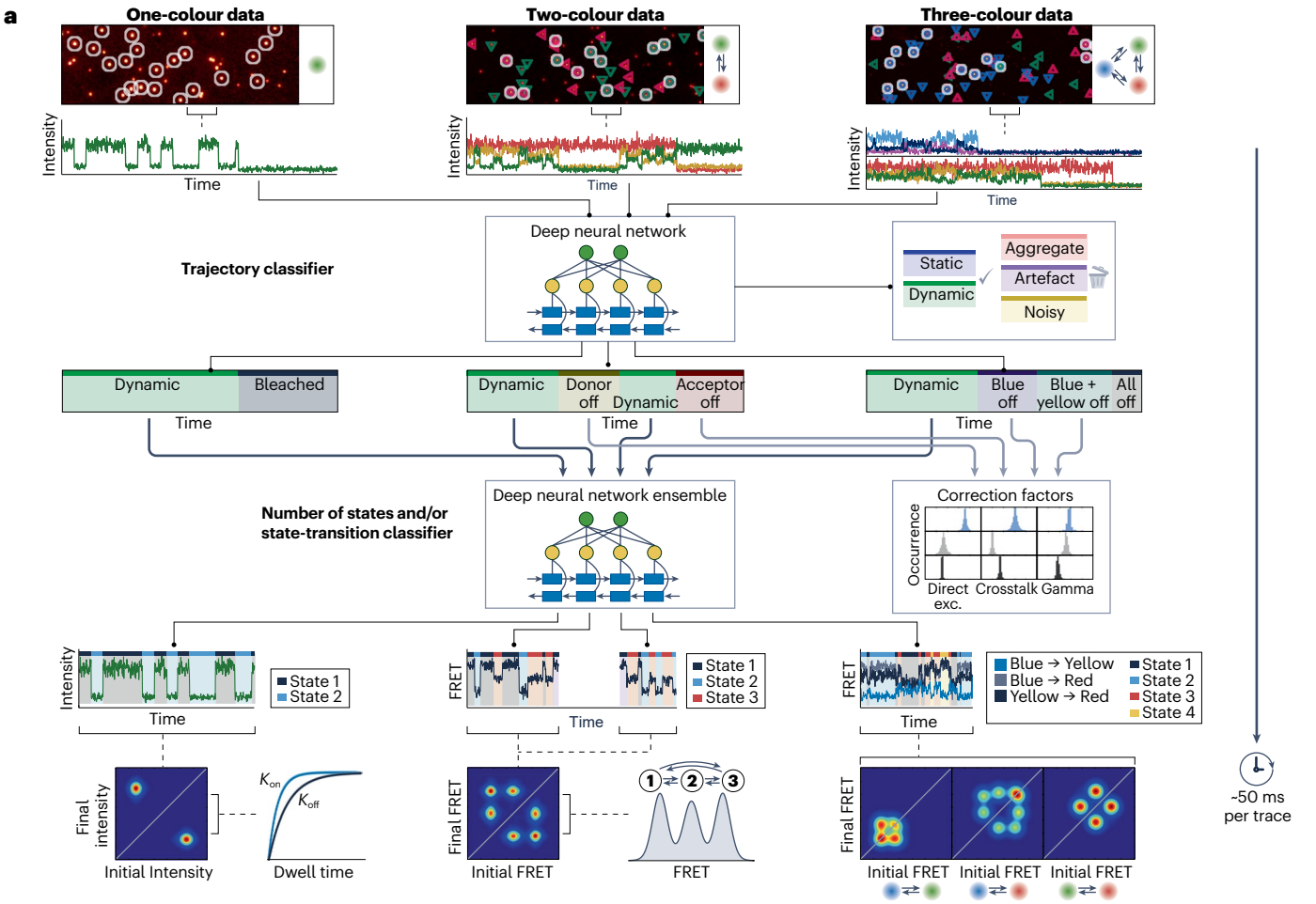
a
One-colour data
Two-colour data
Three-colour data
Intensity
Time
Trajectory classifier
Deep neural network
Static
Dynamic
Aggregate
Artefact
Noisy
Dynamic
Bleached
Donor off
Acceptor off
Blue off
Blue + yellow off
All off
Number of states and/or state-transition classifier
Deep neural network ensemble
Correction factors
Occurrence
Direct exc.
Crosstalk
Gamma
State 1
State 2
State 3
FRET
Blue → Yellow
Blue → Red
Yellow → Red
State 4
Final intensity
Initial Intensity
K_{on}
K_{off}
Dwell time
Final FRET
Initial FRET
FRET
~50 ms per trace
b
All-atom MD
τ_{cd} = 9 ± 2 ns
τ (ns)
2.5 nm
4.0 nm
6.5 nm
90°
P(r)
r (nm)

Fig. 4 | Data analysis and simulations. a, Overview of data extraction, evaluation and analysis using deep-learning-assisted single-molecule imaging analysis[163]. Single-molecule data are identified, extracted, classified into categories and the kinetics and state information evaluated, including the interconversion rates between underlying states[163]. **b**, Example of the direct comparison between simulations and the experiment (Fig. 2c) by generating fluorescence correlation curves based on simulations. Top: nanosecond fluorescence correlation spectroscopy data generated based on the MD simulations with resulting fluorescence intensity correlation times, τ_{cd}. Bottom: snapshots of the configurations of a disordered peptide labelled with donor (green) and acceptor (red) and inter-dye distance distribution from all-atom molecular dynamics (MD) simulations. The agreement with the experimental result (Fig. 2c) indicates that current MD force fields can provide realistic representations of the polypeptide chain dynamics[94]. FRET, Förster resonance energy transfer.

characterize conformations involving high activation barriers, such as the kinetically trapped complex between two RNA hairpins[135], and the kinetic mechanism of DNA double helix dissociation[136]. Notably, as only a small volume is heated, efficient heat dissipation also enables microsecond drops in temperature to be implemented[131]. Developments of this kind will thus increasingly enable the study of conformational states that are so high in free energy that they cannot be observed in equilibrium measurements.

Advances in data analysis and modelling

Although developing new experimental techniques will be essential for extending the scope of single-molecule spectroscopy, going from measurement to conceptual insight requires the quantitative analysis of the data and their interpretation in terms of mechanistic physical models. In the case of single-molecule FRET, this means interpreting a recording of individual photon arrivals in terms of conformational states, their relative populations and their interconversion dynamics (Box 2). Methods for data reduction and analysis in single-molecule experiments have a long history[137,138], and a plethora of techniques and software packages for analysing the rich information contained in single-molecule FRET measurements[19,38,46,139] have been developed see FRET community and refs. 20,140. We will not review the impressive range of established techniques; instead, we will briefly outline some general principles and then focus on a few key developments and future directions that seem particularly promising for enhancing the accessible time resolution and the analysis and interpretation of experiments on complex biomolecular systems.

To take full advantage of the information and time resolution contained in single-molecule fluorescence experiments, and to avoid limitations from time binning, the data are best analysed on a photon-by-photon basis[53]. Time-correlated single-photon counting measurements typically provide for each detected photon its absolute arrival time, the time between exciting laser pulse and emission, its emission wavelength range (that is, whether it was emitted by the donor or the acceptor) and its polarization[38,141]. Arguably, the most versatile framework currently in use for solving the – often challenging – inverse problem of such single-photon recordings is based on likelihood functions, which can be applied to both fluorescence time traces from immobilized molecules and fluorescence bursts from freely diffusing molecules[53]. The likelihood function is essentially (up to a proportionality factor) the joint probability of observing a given photon sequence as a function of the model parameters, most commonly formulated in terms of hidden Markov models[30,50–53]. The model parameters can be inferred by maximizing the likelihood (or log-likelihood) function (Box 3), and their uncertainties can be estimated from the Hessian of the likelihood function at the maximum[142,143]. Many of the established single-molecule analysis methods can ultimately be reduced to this approach.

Applying likelihood-based approaches requires choosing a model. In view of the complexity of biomolecular systems, the number of potential models is vast. Arriving at a physically plausible model thus often needs complementary information. In the case of single-molecule FRET experiments on biomolecules, important information includes the 3D structures of the biomolecules and the known attachment points and chemical structures of the FRET dyes[21]; complementary results from different types of measurements, for example, other spectroscopic techniques[60,144]; effects of photon statistics and the instrumentation on the measurements, such as crosstalk between the detection channels and the instrument response function; and other imperfections, especially fluorescence background or further sources of noise. This information may help to narrow down the number of states observed in the FRET measurements to a reasonable range that can then be included in the hidden Markov models, whose parameters – especially the state-specific emission distributions and the transition rate coefficients between states – are inferred by likelihood maximization, ideally in a global analysis together with other available observables[145]. If several models are plausible, identifying the most suitable yet parsimonious one can be challenging. For models with the same number of parameters, the maximum values of the respective likelihood functions can provide an indication[53]. For models with different numbers of parameters, quantities such as the Bayesian or Akaike information criteria, which penalize overfitting, can be consulted[53,145], but these heuristics are not always conclusive. Other useful ways of differentiating models are the recolouring of the observed photon sequences based on the model[53,146] or simulations of photon emission and comparison with the experimental data[147].

A solution to the current limitations in model selection may be Bayesian nonparametrics[148], a branch of statistics that is only starting to be applied in the physical sciences[149]. With this approach, not only can the parameters of specific preselected models be inferred – or 'learned' – but ideally also the structure of the model itself and the number of states[149–153]. An interesting example of this approach is the recent analysis of freely diffusing molecules that enables both the diffusion coefficients and the number of molecules contributing to emission to be estimated from a small fraction of the data required for traditional FCS[154]. Related developments have been suggested for single-molecule FRET[150,152,153]. Bayesian nonparametrics also allow measurement uncertainties to be propagated rigorously to the uncertainties of the inferred parameters. However, quantifying the requisite measurement uncertainties with sufficient precision often remains challenging[22]. A further current limitation in Bayesian nonparametrics is that sampling the parameter distribution requires computationally expensive numerical schemes, which has limited their application to small data sets. Probing highly heterogeneous systems involving large amounts of data thus continues to benefit from strategies based on the computationally more efficient likelihood maximization[155], as recently demonstrated for protein oligomerization and aggregation in combination with FRET[156].

Another promising research direction is the use of deep learning for single-molecule data analysis and modelling[157]. Recently, first deep-learning-based approaches have been developed for the automation of single-molecule localization as well as fluorescence time trace selection and analysis[158–163] (Fig. 4a). Especially for large data sets with

Glossary

Bayesian nonparametrics
A type of statistical models and methods characterized by large parameter spaces, such as unknown numbers of microstates and their connectivity, and by the construction of probability measures over these spaces.

Chemical kinetics
Description of the time dependence of the interconversion between thermodynamic states and microstates of a system in terms of rates.

Coarse-grained
In modelling complex systems or in renormalization, coarse-graining refers to the procedure in which two or more microscopic entities are replaced with a single entity to reduce the complexity or resolution of the model.

Droplet microfluidics
A method to manipulate discrete, typically picolitre volumes of fluids in immiscible phases. For biomolecules, aqueous droplets in oil are commonly used.

Ensemble average
The mean value of some observables obtained from simultaneous measurements of all members of a statistical ensemble. Single-molecule spectroscopy overcomes ensemble averaging.

Fluorescence correlation spectroscopy
(FCS). Statistical analysis of fluctuations in fluorescence intensity or count rates via time correlation. FCS is a broadly applicable way of assessing biomolecular dynamics over a broad range of timescales.

Förster resonance energy transfer
(FRET). Non-radiative transfer of excitation energy between two molecular entities separated by distances considerably exceeding the sum of their van der Waals radii in the very weak dipole–dipole coupling limit.

Hydrodynamic focusing
A technique used in microfluidics, in which several fluid streams are combined in microfluidic channels to form a layer or jet that is so thin that it exchanges its solutes very rapidly with the neighbouring streams by diffusion.

Local density of optical states
Measures the availability of electromagnetic modes at a given point in space and governs the deexcitation of a quantum emitter.

Multiparameter fluorescence detection
Simultaneous acquisition of multiple fluorescence observables, such as wavelength, count rate, lifetime and anisotropy, as a function of time in a single measurement.

Nanosecond FCS
(ncFCS). Variant of FCS that enables dynamics in the submicrosecond range to be measured by using a Hanbury Brown and Twiss configuration of single-photon detectors.

Photon antibunching
Special distribution of time delays between photons that is characteristic for the emission of a single quantum emitter. Photon antibunching is detected as an anticorrelated component in fluorescence correlation spectroscopy on timescales comparable to the fluorescence lifetime.

Reaction coordinate
A quantity used to describe the progress of a reaction, often chosen to reflect a change in experimental signal. In the context of Förster resonance energy transfer experiments, the reaction coordinate would typically be related to an intramolecular or intermolecular distance change.

Reconfiguration times
Relaxation time of the correlation function of a point-to-point distance within a molecule, most commonly a polymer chain.

Simulation-based inference
Emerging family of methods that infer the model parameters when the likelihood is intractable by integrating simulations with machine learning.

Single-molecule spectroscopy
Methods that enable the physical properties of individual molecules to be measured.

Time average
The mean value of some observables obtained from measurements of an individual member of the ensemble as a function of time, for example, as a result of time binning. Single-molecule spectroscopy overcomes time averaging for processes that can be resolved with the time resolution of the specific measurement.

Transition paths
The successful reactant-to-product crossing of the free-energy barrier separating two free-energy minima. Transition paths are rare events with very short duration and thus challenging to resolve experimentally.

thousands of traces, manual selection becomes prohibitive. Neural networks trained with large experimental and/or simulated data sets based on Markov state models can greatly accelerate the selection of time traces to eliminate recordings that exhibit undesired contributions, such as sample aggregation, uncorrelated donor–acceptor signal, photochemical artefacts or low signal to noise. Automated classification not only accelerates throughput but may also increase reproducibility by reducing user bias. Deep neural networks can further be used to rapidly analyse single-molecule FRET data, including the number of states, interconversion kinetics and trace-specific correction factors for direct acceptor excitation, crosstalk and detection efficiencies, even for three-colour FRET experiments[163] (Fig. 4a). An added advantage is that the number of states required for describing the data and their connectivity do not have to be preselected if either the training set is sufficiently comprehensive[163] or unsupervised learning is used[161,164], thus providing a powerful way of identifying candidate models. Deep-learning-based methods so far have been based on time-binned data, but the extension to single-photon data might open up an opportunity for optimizing the analysis of very fast processes or very large data sets for which likelihood-based and nonparametric techniques are not computationally feasible. The increasing availability of entry-level platforms for training deep learning networks[165] is likely to accelerate this process.

Combining single-molecule FRET and molecular simulations

Many questions, however, are difficult to formulate in terms of descriptions as simple as Markov state models, and more detailed molecular models are required, such as atomistic or coarse-grained simulations. An exciting development of the past decade is the increasing overlap between timescales accessible in molecular dynamics simulations and biophysical experiments[166], including single-molecule spectroscopy. Comparing absolute timescales of biomolecular dynamics between experiment and simulation usually requires atomistic molecular dynamics simulations, including an explicit representation of the solvent. Atomistic detail helps account for all internal degrees of freedom,

enabling a faithful description of dissipative forces such as friction in terms of random collisions and interactions at the molecular level. Such simulations are now feasible up to the millisecond range, and the force fields have reached a level of accuracy that allows processes such as the folding of small proteins to be simulated in remarkable agreement with experimental data[167,168]. Even the routinely accessible microsecond range provides ample opportunity for comparisons with the rapid dynamics that can be measured with single-molecule FRET, including transition path times of protein folding[169], polypeptide chain dynamics[94] and biomolecular phase separation[170], to name but a few.

To directly compare with the experimentally observed statistics of photon emission, simulations must include the FRET dyes explicitly[171]. A Monte Carlo scheme based on the distance between donor and acceptor, their relative orientation at every time step and the known photophysics of the FRET process can then be used[172,173]. Note that a faithful representation of the interactions of the fluorophores with the biomolecule usually requires the dedicated optimization of force field parameters, for example, by direct comparison with time-resolved fluorescence anisotropy measurements[174–176]. Figure 3b shows a recent example of combining single-molecule spectroscopy with molecular dynamics simulations: Nüesch et al.[94] used plasmonic enhancement in ZMWs to increase the time resolution of nsFCS in the low nanosecond range to measure the chain dynamics of short peptides (Fig. 2c). They compared the resulting correlation functions with microsecond molecular dynamics simulations of the system including fluorophores (Fig. 3b). The agreement between measured and simulated distance distributions and dynamics suggests that the accuracy of such simulations has reached a stage where they enable a quantitative mechanistic interpretation of single-molecule FRET experiments, including the influence of the fluorophores. Experimental benchmarking of simulations has in turn developed into an essential strategy for force field optimization[174,177–180] and the reweighting of subtrajectories from extensive molecular dynamics simulations[181,182].

Such simulations have thus become an important strategy for providing a physical model and a mechanistic interpretation of single-molecule FRET experiments. For many biomolecular systems, however, fully atomistic simulations are not feasible even with the world's most powerful supercomputers, either because of the large size of the molecules or the long timescales of interest. In such situations, coarse-grained models, in which faster degrees of freedom are effectively integrated out, provide a valuable alternative[183,184]. In a popular type of model, several atoms are combined in a single bead; the bead sizes and chain connectivity are defined based on the known chemical structure; and non-covalent interactions are described by combining Debye–Hückel-type electrostatics, Lennard–Jones-type short-range potentials and structure-based potentials[62,185–187]. The simulations are computationally much cheaper and thus allow the dynamics of even large biomolecular complexes to be sampled efficiently[63,188,189]; moreover, the simplicity of the model enables the optimization of the potential based on direct comparison with experimental data[187,190,191], for instance, by globally adjusting the energy scale of the short-range interactions to match experimentally observed transfer efficiencies[62,188,192]. Although this approach yields physically plausible conformational ensembles, the removal of molecular degrees of freedom and the softer interaction potentials compared with all-atom representations lead to lower frictional forces and reduced barrier heights, which distort the relative timescales of different dynamical processes[193]. Experimental and simulated dynamics can be compared semi-quantitatively by the empirical rescaling of time[192,194], but the development of more sophisticated approaches for coarse-grained biomolecular dynamics is an important direction of future research[193].

Simulation-based inference[195] is an exciting emerging combination of simulations and machine learning. As we have seen, various methods are available for simulating the behaviour of biomolecules and generating synthetic data, including photon emission, and comparing them directly with single-molecule FRET measurements. Ideally, this comparison should enable the parameters of the simulation model to be learnt based on a likelihood function. However, in contrast to simple Markov state models, the likelihood functions are often not tractable, because they are only implicitly encoded by the model and essentially correspond to an integral over all possible trajectories given a set of parameters. Recent developments in simulation-based inference may change this situation by incorporating surrogate models based on deep neural networks, active learning — the idea of continuously using the acquired knowledge to guide sampling — and the modification of the simulation code during the inference workflow[195]. First applications to single-molecule data are the simulation-based inference of molecular potentials from force spectroscopy[196] and the classification of diffusive trajectories of protein molecules in neurons[197]. Applying these ideas to more complex molecular simulation models may soon be within reach, which could have a profound impact on how we establish detailed models of biomolecular dynamics based on single-molecule FRET and other experiments.

Conclusions and outlook

Single-molecule FRET now has a firm place in the repertoire of biological physics, but even after almost 30 years since its inception[16], the method continues to enable new developments and synergies. These developments have enabled us to probe the nanoscale motions of biomolecules across a vast range of timescales, from nanoseconds to hours or even days. Advances in nanophotonics have started to facilitate access to the nanosecond range and may soon enable us to resolve even rapid rare events, such as transition paths across free-energy barriers. A growing tool box of physics-based techniques allows us to extend biophysical investigations to processes out of equilibrium. Impressive advances in data analysis techniques enable an increasingly rigorous and complete interpretation of multiparameter fluorescence data. Molecular simulations have been reaching the level of accuracy required for predictive power, and the increasing overlap between the timescales of simulations and experiment provides the exciting opportunity of direct comparison between the two. Finally, recent breakthroughs in deep learning are likely to yield unexpected new analysis techniques and novel ways of linking simulation and experiment.

In this Review, we have only been able to touch on some of the exciting research directions that are currently being taken, but many other promising recent advances would be worth mentioning. Among these are combinations of FRET with powerful complementary techniques, such as optical or magnetic tweezers for monitoring forces[49,198] and FRET on single molecules simultaneously[199]; anti-Brownian electrokinetic trapping for observing individual molecules for minutes without surface-tethering[200,201]; techniques for high-pressure studies[202,203]; new detector technologies such as SPAD[204] and nanowire arrays for multifocal detection; the integration of fluorescence detection with interferometric scattering[205]; temperature-cycle microscopy, in which the sample is switched between the solid and liquid state by laser temperature jumps and rapid freezing on the microsecond timescale[206]; innovative strategies for increasing

the fluorescence detection efficiency from single molecules, such as optofluidic antennas[207]; the combination of FRET with optical super-resolution techniques[208]; and approaches that enable single-molecule FRET inside live cells[28,209]. Clever data analysis methods also continue to be advanced, such as the powerful extension of burst variance analysis to a time-resolved variant for probing microsecond and millisecond dynamics[210]; the quantitative analysis of steady-state kinetics far from equilibrium[211]; the detection of non-Markov dynamics based on information theory[212]; or the systematic and global analysis of transfer efficiencies, fluorescence lifetimes, photon distribution analysis and correlation functions[213,214].

Achieving the goal of understanding biomolecular dynamics will of course also benefit from single-molecule approaches other than FRET[215]. Examples are the use of processes that affect the fluorescence signal but are unrelated to Förster transfer, such as changes in quantum yield when certain fluorophores interact with the surface of a biomolecule (termed protein-induced[216] or photoisomerization-related fluorescence enhancement[217]). Fluorescence quenching by photoinduced electron transfer, which requires van der Waals contact between two chromophores, can be used to probe short-range dynamics[218,219]. Another exciting opportunity is the use of complementary methods that enable distance measurements at the nanometre scale, such as cryogenic localization microscopy[220] or MINFLUX[221]. Finally, there is a broad range of elegant single-molecule force spectroscopy methods to probe the mechanical properties of individual biomolecules[49,198]. In summary, there is ample opportunity for using experimental and theoretical physics to advance our capabilities of probing the behaviour and function of biomolecules at the single-molecule level. These advances will not only allow us to understand molecular dynamics in increasingly complex biological systems and environments but also hold great promise for extending the scope of single-molecule techniques to other areas of soft-matter physics, such as synthetic polymers and colloids[222].

Published online: 12 September 2024

References

1. Tanford, C. & Reynolds, J. *Nature's Robots: A History of Proteins* (Oxford Univ. Press, 2003).
2. Berman, H. M. et al. The Protein Data Bank. *Nucleic Acids Res.* **28**, 235–242 (2000).
3. Benson, D. A. et al. GenBank. *Nucleic Acids Res.* **42**, D32–D37 (2014).
4. Jumper, J. et al. Highly accurate protein structure prediction with AlphaFold. *Nature* **596**, 583–589 (2021).
5. McCammon, J. A. & Harvey, S. C. *Dynamics of Proteins and Nucleic Acids* (Cambridge Univ. Press, 1988).
6. Frauenfelder, H., Sligar, S. G. & Wolynes, P. G. The energy landscapes and motions of proteins. *Science* **254**, 1598–1603 (1991).
7. Haran, G. & Riven, I. Perspective: how fast dynamics affect slow function in protein machines. *J. Phys. Chem. B* **127**, 4687–4693 (2023).
8. Bahar, I., Jernigan, R. & Dill, K. A. *Protein Actions: Principles and Modeling* (Garland Science, Taylor & Francis Group, 2017).
9. Jaenicke, R. Protein folding. In *Proc. 28th Conf. German Biochemical Society, University of Regensburg, Regensburg, West Germany,* 10–12 September 1979 (Elsevier, 1980).
10. Fersht, A. *Structure and Mechanism in Protein Science: A Guide to Enzyme Catalysis and Protein Folding* (World Scientific, 2017).
11. van der Lee, R. et al. Classification of intrinsically disordered regions and proteins. *Chem. Rev.* **114**, 6589–6631 (2014).
12. Kulzer, F. & Orrit, M. Single-molecule optics. *Annu. Rev. Phys. Chem.* **55**, 585–611 (2004).
13. Moerner, W. E. A dozen years of single-molecule spectroscopy in physics, chemistry, and biophysics. *J. Phys. Chem. B* **106**, 910–927 (2002).
14. Gräslund, A., Rigler, R. & Widengren, J. *Single Molecule Spectroscopy in Chemistry, Physics and Biology* Vol. 96 (Springer, 2010).
15. Makarov, D. E. *Single Molecule Science — Physical Principles and Models* (CRC Press, 2015).
16. Ha, T. et al. Probing the interaction between two single molecules: fluorescence resonance energy transfer between a single donor and a single acceptor. *Proc. Natl Acad. Sci. USA* **93**, 6264–6268 (1996).
17. Stryer, L. Fluorescence energy transfer as a spectroscopic ruler. *Annu. Rev. Biochem.* **47**, 819–846 (1978).
18. Förster, T. Zwischenmolekulare Energiewanderung und Fluoreszenz. *Ann. Phys.-Berl.* **6**, 55–75 (1948).
19. Joo, C., Balci, H., Ishitsuka, Y., Buranachai, C. & Ha, T. Advances in single-molecule fluorescence methods for molecular biology. *Annu. Rev. Biochem.* **77**, 51–76 (2008).
20. Lerner, E. et al. FRET-based dynamic structural biology: challenges, perspectives and an appeal for open-science practices. *eLife* **10**, e60416 (2021).
21. Dimura, M. et al. Quantitative FRET studies and integrative modeling unravel the structure and dynamics of biomolecular systems. *Curr. Opin. Struct. Biol.* **40**, 163–185 (2016).
22. Hellenkamp, B. et al. Precision and accuracy of single-molecule FRET measurements — a multi-laboratory benchmark study. *Nat. Methods* **15**, 669–676 (2018).
23. Agam, G. et al. Reliability and accuracy of single-molecule FRET studies for characterization of structural dynamics and distances in proteins. *Nat. Methods* **20**, 523–535 (2023).
24. Lemke, E. A. Site-specific labeling of proteins for single-molecule FRET measurements using genetically encoded ketone functionalities. *Methods Mol. Biol.* **751**, 3–15 (2011).
25. Zosel, F., Holla, A. & Schuler, B. Labeling of proteins for single-molecule fluorescence spectroscopy. *Methods Mol. Biol.* **2376**, 207–233 (2022).
26. Ha, T. & Tinnefeld, P. Photophysics of fluorescent probes for single-molecule biophysics and super-resolution imaging. *Annu. Rev. Phys. Chem.* **63**, 595–617 (2012).
27. Campos, L. A. et al. A photoprotection strategy for microsecond-resolution single-molecule fluorescence spectroscopy. *Nat. Methods* **8**, 143–146 (2011).
28. Sustarsic, M. & Kapanidis, A. N. Taking the ruler to the jungle: single-molecule FRET for understanding biomolecular structure and dynamics in live cells. *Curr. Opin. Struct. Biol.* **34**, 52–59 (2015).
29. Schuler, B. & Hofmann, H. Single-molecule spectroscopy of protein folding dynamics — expanding scope and timescales. *Curr. Opin. Struct. Biol.* **23**, 36–47 (2013).
30. Mazal, H. & Haran, G. Single-molecule FRET methods to study the dynamics of proteins at work. *Curr. Opin. Biomed. Eng.* **12**, 8–17 (2019).
31. Michalet, X. et al. Detectors for single-molecule fluorescence imaging and spectroscopy. *J. Mod. Opt.* **54**, 239 (2007).
32. Selvin, P. R. & Ha, T. *Single-Molecule Techniques: A Laboratory Manual* (Cold Spring Harbor Laboratory Press, 2008).
33. Juette, M. F. et al. Single-molecule imaging of non-equilibrium molecular ensembles on the millisecond timescale. *Nat. Methods* **13**, 341–344 (2016).
34. Pati, A. K. et al. Tuning the Baird aromatic triplet-state energy of cyclooctatetraene to maximize the self-healing mechanism in organic fluorophores. *Proc. Natl Acad. Sci. USA* **117**, 24305–24315 (2020).
35. Bronzi, D., Villa, F., Tisa, S., Tosi, A. & Zappa, F. SPAD figures of merit for photon-counting, photon-timing, and imaging applications: a review. *IEEE Sens. J.* **16**, 3–12 (2016).
36. Brand, L., Eggeling, C., Zander, C., Drexhage, K. H. & Seidel, C. A. M. Single-molecule identification of Coumarin-120 by time-resolved fluorescence detection: comparison of one- and two-photon excitation in solution. *J. Phys. Chem. A* **101**, 4313–4321 (1997).
37. Vermeer, B. & Schmid, S. Can DyeCycling break the photobleaching limit in single-molecule FRET? *Nano Res.* **15**, 9818–9830 (2022).
38. Sisamakis, E., Valeri, A., Kalinin, S., Rothwell, P. J. & Seidel, C. A. M. Accurate single-molecule FRET studies using multiparameter fluorescence detection. *Methods Enzymol.* **475**, 455–514 (2010).
39. Gambin, Y. & Deniz, A. A. Multicolor single-molecule FRET to explore protein folding and binding. *Mol. Biosyst.* **6**, 1540–1547 (2010).
40. Götz, M., Wortmann, P., Schmid, S. & Hugel, T. A multicolor single-molecule FRET approach to study protein dynamics and interactions simultaneously. *Methods Enzymol.* **581**, 487–516 (2016).
41. Van Der Meer, B. W., Coker, G. III & Chen, S. Y. S. *Resonance Energy Transfer: Theory and Data* (VCH Publishers, Inc., 1994).
42. Kurtsiefer, C., Zarda, P., Mayer, S. & Weinfurter, H. The breakdown flash of silicon avalanche photodiodes — back door for eavesdropper attacks? *J. Mod. Opt.* **48**, 2039–2047 (2001).
43. Nettels, D., Gopich, I. V., Hoffmann, A. & Schuler, B. Ultrafast dynamics of protein collapse from single-molecule photon statistics. *Proc. Natl Acad. Sci. USA* **104**, 2655–2660 (2007).
44. Kudryavtsev, V. et al. Combining MFD and PIE for accurate single-pair Förster resonance energy transfer measurements. *ChemPhysChem* **13**, 1060–1078 (2012).
45. Schuler, B., Soranno, A., Hofmann, H. & Nettels, D. Single-molecule FRET spectroscopy and the polymer physics of unfolded and intrinsically disordered proteins. *Annu. Rev. Biophys.* **45**, 207–231 (2016).
46. Lerner, E. et al. Toward dynamic structural biology: two decades of single-molecule Förster resonance energy transfer. *Science* **359**, eaan1133 (2018).
47. Hänggi, P., Talkner, P. & Borkovec, M. Reaction-rate theory — fifty years after Kramers. *Rev. Mod. Phys.* **62**, 251–341 (1990).
48. Chung, H. S. & Eaton, W. A. Protein folding transition path times from single molecule FRET. *Curr. Opin. Struct. Biol.* **48**, 30–39 (2018).
49. Hoffer, N. Q. & Woodside, M. T. Probing microscopic conformational dynamics in folding reactions by measuring transition paths. *Curr. Opin. Chem. Biol.* **53**, 68–74 (2019).
50. McKinney, S. A., Joo, C. & Ha, T. Analysis of single-molecule FRET trajectories using hidden Markov modeling. *Biophys. J.* **91**, 1941–1951 (2006).
51. Talaga, D. S. Markov processes in single molecule fluorescence. *Curr. Opin. Colloid* **12**, 285–296 (2007).

52. Pirchi, M. et al. Photon-by-photon hidden Markov model analysis for microsecond single-molecule FRET kinetics. *J. Phys. Chem. B* **120**, 13065–13075 (2016).
53. Gopich, I. V. & Chung, H. S. Theory and analysis of single-molecule FRET experiments. *Methods Mol. Biol.* **2376**, 247–282 (2022).
54. Rigler, R. & Elson, E. S. *Fluorescence Correlation Spectroscopy: Theory and Applications* (Springer, 2001).
55. Zander, C., Enderlein, J. & Keller, R. A. *Single Molecule Detection in Solution* (Wiley-VCH, 2002).
56. Ghosh, A. & Enderlein, J. Advanced fluorescence correlation spectroscopy for studying biomolecular conformation. *Curr. Opin. Struct. Biol.* **70**, 123–131 (2021).
57. Felekyan, S., Kalinin, S., Sanabria, H., Valeri, A. & Seidel, C. A. M. Filtered FCS: species auto- and cross-correlation functions highlight binding and dynamics in biomolecules. *ChemPhysChem* **13**, 1036–1053 (2012).
58. Kapusta, P., Wahl, M., Benda, A., Hof, M. & Enderlein, J. Fluorescence lifetime correlation spectroscopy. *J. Fluoresc.* **17**, 43–48 (2007).
59. Soranno, A. et al. Quantifying internal friction in unfolded and intrinsically disordered proteins with single molecule spectroscopy. *Proc. Natl Acad. Sci. USA* **109**, 17800–17806 (2012).
60. Schuler, B. et al. Binding without folding — the biomolecular function of disordered polyelectrolyte complexes. *Curr. Opin. Struct. Biol.* **60**, 66–76 (2019).
61. Fuxreiter, M. & Tompa, P. Fuzziness: structural disorder in protein complexes. *Trends Biochem. Sci.* **33**, 2–8 (2012).
62. Borgia, A. et al. Extreme disorder in an ultrahigh-affinity protein complex. *Nature* **555**, 61–66 (2018).
63. Wiggers, F. et al. Diffusion of a disordered protein on its folded ligand. *Proc. Natl Acad. Sci. USA* **118**, e2106690118 (2021).
64. Sauer, M., Hofkens, J. & Enderlein, J. *Handbook of Fluorescence Spectroscopy and Imaging: From Single Molecules to Ensembles*.(Wiley-VCH, 2011).
65. Hübner, C. G. et al. Photon antibunching and collective effects in the fluorescence of single bichromophoric molecules. *Phys. Rev. Lett.* **91**, 093903 (2003).
66. Chung, H. S., Louis, J. M. & Eaton, W. A. Experimental determination of upper bound for transition path times in protein folding from single-molecule photon-by-photon trajectories. *Proc. Natl. Acad. Sci. USA* **106**, 11837–11844 (2009).
67. Chung, H. S., McHale, K., Louis, J. M. & Eaton, W. A. Single-molecule fluorescence experiments determine protein folding transition path times. *Science* **335**, 981–984 (2012).
68. Giannini, V., Fernandez-Dominguez, A. I., Heck, S. C. & Maier, S. A. Plasmonic nanoantennas: fundamentals and their use in controlling the radiative properties of nanoemitters. *Chem. Rev.* **111**, 3888–3912 (2011).
69. Purcell, E. M. Spontaneous emission probabilities at radio frequencies. *Phys. Rev.* **69**, 681–681 (1946).
70. Barnes, W. L., Horsley, S. A. R. & Vos, W. L. Classical antennas, quantum emitters, and densities of optical states. *J. Optics* **22**, 073501 (2020).
71. Dirac, P. A. M. The quantum theory of the emission and absorption of radiation. *Proc. R. Soc. Lond. A* **114**, 243–265 (1927).
72. Andrew, P. & Barnes, W. L. Förster energy transfer in an optical microcavity. *Science* **290**, 785–788 (2000).
73. Barnes, W. L. Fluorescence near interfaces: the role of photonic mode density. *J. Mod. Opt.* **45**, 661–699 (1998).
74. Gregor, I., Chizhik, A., Karedla, N. & Enderlein, J. Metal-induced energy transfer. *Nanophotonics* **8**, 1689–1699 (2019).
75. Chhabra, R. et al. Distance-dependent interactions between gold nanoparticles and fluorescent molecules with DNA as tunable spacers. *Nanotechnology* **20**, 485201 (2009).
76. Seelig, J. et al. Nanoparticle-induced fluorescence lifetime modification as nanoscopic ruler: demonstration at the single molecule level. *Nano Lett.* **7**, 685–689 (2007).
77. Acuna, G. P. et al. Distance dependence of single-fluorophore quenching by gold nanoparticles studied on DNA origami. *ACS Nano* **6**, 3189–3195 (2012).
78. Novotny, L. & Hecht, B. *Principles of Nano-Optics* (Cambridge Univ. Press, 2006).
79. Drexhage, K. H. Influence of a dielectric interface on fluorescence decay time. *J. Lumin.* **1–2**, 693–701 (1970).
80. Maccaferri, N. et al. Recent advances in plasmonic nanocavities for single-molecule spectroscopy. *Nanoscale Adv.* **3**, 633–642 (2021).
81. Acuna, G. P. et al. Fluorescence enhancement at docking sites of DNA-directed self-assembled nanoantennas. *Science* **338**, 506–510 (2012).
82. Glembockyte, V., Grabenhorst, L., Trofymchuk, K. & Tinnefeld, P. DNA origami nanoantennas for fluorescence enhancement. *Acc. Chem. Res.* **54**, 3338–3348 (2021).
83. Liu, N. & Liedl, T. DNA-assembled advanced plasmonic architectures. *Chem. Rev.* **118**, 3032–3053 (2018).
84. Grabenhorst, L., Sturzenegger, F., Hasler, M., Schuler, B. & Tinnefeld, P. Single-molecule FRET at 10 MHz count rates. *J. Am. Chem. Soc.* **146**, 3539–3544 (2024).
85. Levene, M. J. et al. Zero-mode waveguides for single-molecule analysis at high concentrations. *Science* **299**, 682–686 (2003).
86. Bethe, H. A. Theory of diffraction by small holes. *Phys. Rev.* **66**, 163–182 (1944).
87. Punj, D. et al. Plasmonic antennas and zero-mode waveguides to enhance single molecule fluorescence detection and fluorescence correlation spectroscopy toward physiological concentrations. *Wires Nanomed. Nanobiotechnol.* **6**, 268–282 (2014).
88. Eid, J. et al. Real-time DNA sequencing from single polymerase molecules. *Science* **323**, 133–138 (2009).
89. Rigneault, H. et al. Enhancement of single-molecule fluorescence detection in subwavelength apertures. *Phys. Rev. Lett.* **95**, 117401 (2005).
90. Baibakov, M. et al. Extending single-molecule Förster resonance energy transfer (FRET) range beyond 10 nanometers in zero-mode waveguides. *ACS Nano* **13**, 8469–8480 (2019).
91. de Torres, J., Ghenuche, P., Moparthi, S. B., Grigoriev, V. & Wenger, J. FRET enhancement in aluminum zero-mode waveguides. *ChemPhysChem* **16**, 782–788 (2015).
92. Baibakov, M., Patra, S., Claude, J. B. & Wenger, J. Long-range single-molecule Förster resonance energy transfer between Alexa dyes in zero-mode waveguides. *ACS Omega* **5**, 6947–6955 (2020).
93. Patra, S., Claude, J. B. & Wenger, J. Fluorescence brightness, photostability, and energy transfer enhancement of immobilized single molecules in zero-mode waveguide nanoapertures. *ACS Photon.* **9**, 2109–2118 (2022).
94. Nüesch, M. F. et al. Single-molecule detection of ultrafast biomolecular dynamics with nanophotonics. *J. Am. Chem. Soc.* **144**, 52–56 (2022).
95. Mothi, N. & Muñoz, V. Protein folding dynamics as diffusion on a free energy surface: rate equation terms, transition paths, and analysis of single-molecule photon trajectories. *J. Phys. Chem. B* **125**, 12413–12425 (2021).
96. Kim, J. Y., Meng, F., Yoo, J. & Chung, H. S. Diffusion-limited association of disordered protein by non-native electrostatic interactions. *Nat. Commun.* **9**, 4707 (2018).
97. Sturzenegger, F. et al. Transition path times of coupled folding and binding reveal the formation of an encounter complex. *Nat. Commun.* **9**, 4708 (2018).
98. Kim, J. Y. & Chung, H. S. Disordered proteins follow diverse transition paths as they fold and bind to a partner. *Science* **368**, 1253–1257 (2020).
99. de Torres, J. et al. Plasmonic nanoantennas enable forbidden Förster dipole–dipole energy transfer and enhance the FRET efficiency. *Nano Lett.* **16**, 6222–6230 (2016).
100. Baibakov, M. et al. Zero-mode waveguides can be made better: fluorescence enhancement with rectangular aluminum nanoapertures from the visible to the deep ultraviolet. *Nanoscale Adv.* **2**, 4153–4160 (2020).
101. Natarajan, C. M., Tanner, M. G. & Hadfield, R. H. Superconducting nanowire single-photon detectors: physics and applications. *Supercond. Sci. Tech.* **25**, 063001 (2012).
102. Steinfeld, J. I., Francisco, J. S. & Hase, W. L. *Chemical Kinetics and Dynamics* 2nd edn (Prentice Hall, Inc., 1999).
103. Lee, C. Y., Chang, C. L., Wang, Y. N. & Fu, L. M. Microfluidic mixing: a review. *Int. J. Mol. Sci.* **12**, 3263–3287 (2011).
104. Streets, A. M. & Huang, Y. Microfluidics for biological measurements with single-molecule resolution. *Curr. Opin. Biotechnol.* **25**, 69–77 (2014).
105. Knight, J. B., Vishwanath, A., Brody, J. P. & Austin, R. H. Hydrodynamic focusing on a silicon chip: mixing nanoliters in microseconds. *Phys. Rev. Lett.* **80**, 3863–3866 (1998).
106. Brody, J. P., Yager, P., Goldstein, R. E. & Austin, R. H. Biotechnology at low Reynolds numbers. *Biophys. J.* **71**, 3430–3441 (1996).
107. Dimotakis, P. E. Turbulent mixing. *Annu. Rev. Fluid Mech.* **37**, 329–356 (2005).
108. Wunderlich, B. et al. Microfluidic mixer designed for performing single-molecule kinetics with confocal detection on timescales from milliseconds to minutes. *Nat. Protoc.* **8**, 1459–1474 (2013).
109. Pfeil, S. H., Wickersham, C. E., Hoffmann, A. & Lipman, E. A. A microfluidic mixing system for single-molecule measurements. *Rev. Sci. Instrum.* **80**, 055105 (2009).
110. Yao, S. & Bakajin, O. Improvements in mixing time and mixing uniformity in devices designed for studies of protein folding kinetics. *Anal. Chem.* **79**, 5753–5759 (2007).
111. Hertzog, D. E. et al. Femtomole mixer for microsecond kinetic studies of protein folding. *Anal. Chem.* **76**, 7169–7178 (2004).
112. Lipman, E. A., Schuler, B., Bakajin, O. & Eaton, W. A. Single-molecule measurement of protein folding kinetics. *Science* **301**, 1233–1235 (2003).
113. Hamadani, K. M. & Weiss, S. Nonequilibrium single molecule protein folding in a coaxial mixer. *Biophys. J.* **95**, 352–365 (2008).
114. Gambin, Y. et al. Visualizing a one-way protein encounter complex by ultrafast single-molecule mixing. *Nat. Methods* **8**, 239–241 (2011).
115. Orte, A., Craggs, T. D., White, S. S., Jackson, S. E. & Klenerman, D. Evidence of an intermediate and parallel pathways in protein unfolding from single-molecule fluorescence. *J. Am. Chem. Soc.* **130**, 7898–7907 (2008).
116. Borgia, A. et al. Localizing internal friction along the reaction coordinate of protein folding by combining ensemble and single molecule fluorescence spectroscopy. *Nat. Commun.* **2**, 1195 (2012).
117. Soranno, A. et al. Integrated view of internal friction in unfolded proteins from single-molecule FRET, contact quenching, theory, and simulations. *Proc. Natl Acad. Sci. USA* **114**, E1833–E1839 (2017).
118. Dingfelder, F. et al. Slow escape from a helical misfolded state of the pore-forming toxin cytolysin A. *JACS Au* **1**, 1217–1230 (2021).
119. Zijlstra, N. et al. Rapid microfluidic dilution for single-molecule spectroscopy of low-affinity biomolecular complexes. *Angew. Chem. Int. Ed. Engl.* **56**, 7126–7129 (2017).
120. Hellenkamp, B., Thurn, J., Stadlmeier, M. & Hugel, T. Kinetics of transient protein complexes determined via diffusion-independent microfluidic mixing and fluorescence stoichiometry. *J. Phys. Chem. B* **122**, 11554–11560 (2018).
121. Dingfelder, F. et al. Rapid microfluidic double-jump mixing device for single-molecule spectroscopy. *J. Am. Chem. Soc.* **139**, 6062–6065 (2017).
122. *Droplet Microfluidics* Vol. 12 (The Royal Society of Chemistry, 2021).
123. Song, H., Bringer, M. R., Tice, J. D., Gerdts, C. J. & Ismagilov, R. F. Experimental test of scaling of mixing by chaotic advection in droplets moving through microfluidic channels. *Appl. Phys. Lett.* **83**, 4664–4666 (2003).

124. Yang, T. et al. Rapid droplet-based mixing for single-molecule spectroscopy. *Nat. Methods* **20**, 1479–1482 (2023).
125. Beard, D. A. Taylor dispersion of a solute in a microfluidic channel. *J. Appl. Phys.* **89**, 4667–4669 (2001).
126. Wunderlich, B., Nettels, D. & Schuler, B. Taylor dispersion and the position-to-time conversion in microfluidic mixing devices. *Lab Chip* **14**, 219–228 (2014).
127. Charmet, J., Arosio, P. & Knowles, T. P. J. Microfluidics for protein biophysics. *J. Mol. Biol.* **430**, 565–580 (2018).
128. Benke, S. et al. Combining rapid microfluidic mixing and three-color single-molecule FRET for probing the kinetics of protein conformational changes. *J. Phys. Chem. B* **125**, 6617–6628 (2021).
129. Barth, A., Voith von Voithenberg, L. & Lamb, D. C. Quantitative single-molecule three-color Förster resonance energy transfer by photon distribution analysis. *J. Phys. Chem. B* **123**, 6901–6916 (2019).
130. Yang, T. et al. Droplet-based microfluidic temperature-jump platform for the rapid assessment of biomolecular kinetics. *Anal. Chem.* **94**, 16675–16684 (2022).
131. Polinkovsky, M. E. et al. Ultrafast cooling reveals microsecond-scale biomolecular dynamics. *Nat. Commun.* **5**, 5737 (2014).
132. Abate, A. R., Hung, T., Mary, P., Agresti, J. J. & Weitz, D. A. High-throughput injection with microfluidics using picoinjectors. *Proc. Natl Acad. Sci. USA* **107**, 19163–19166 (2010).
133. Liao, D. et al. Single molecule correlation spectroscopy in continuous flow mixers with zero-mode waveguides. *Opt. Expr.* **16**, 10077–10090 (2008).
134. Holmstrom, E. D. & Nesbitt, D. J. Real-time infrared overtone laser control of temperature in picoliter H_2O samples: 'nanobathtubs' for single molecule microscopy. *J. Phys. Chem. Lett.* **1**, 2264–2268 (2010).
135. Zhao, R. et al. Laser-assisted single-molecule refolding (LASR). *Biophys. J.* **99**, 1925–1931 (2010).
136. Holmstrom, E. D., Dupuis, N. F. & Nesbitt, D. J. Pulsed IR heating studies of single-molecule DNA duplex dissociation kinetics and thermodynamics. *Biophys. J.* **106**, 220–231 (2014).
137. Sakmann, B. & Neher, E. *Single Channel Recording* (Plenum Press, 1995).
138. Barkai, E., Brown, F. L. H., Orrit, M. & Yang, H. *Theory and Evaluation of Single-Molecule Signals* (World Scientific Pub., Co., 2009).
139. Tavakoli, M., Taylor, J. N., Li, C. B., Komatsuzaki, T. & Pressé, S. Single molecule data analysis: an introduction. *Adv. Chem. Phys.* **162**, 205–305 (2017).
140. Götz, M. et al. A blind benchmark of analysis tools to infer kinetic rate constants from single-molecule FRET trajectories. *Nat. Commun.* **13**, 5402 (2022).
141. Chowdhury, A., Nettels, D. & Schuler, B. Interaction dynamics of intrinsically disordered proteins from single-molecule spectroscopy. *Annu. Rev. Biophys.* **52**, 433–62 (2023).
142. Gopich, I. V. Accuracy of maximum likelihood estimates of a two-state model in single-molecule FRET. *J. Chem. Phys.* **142**, 034110 (2015).
143. D'Agostini, G. *Bayesian Reasoning in Data Analysis: A Critical Introduction* (World Scientific, 2003).
144. Schanda, P. & Haran, G. NMR and smFRET insights into fast protein motions and their relation to function. *Annu. Rev. Biophys.* **53**, 247–273 (2024).
145. Kinz-Thompson, C. D., Ray, K. K. & Gonzalez, R. L. Jr. Bayesian inference: the comprehensive approach to analyzing single-molecule experiments. *Annu. Rev. Biophys.* **50**, 191–208 (2021).
146. Gopich, I. V. & Szabo, A. Decoding the pattern of photon colors in single-molecule FRET. *J. Phys. Chem. B* **113**, 10965–10973 (2009).
147. Zosel, F., Mercadante, D., Nettels, D. & Schuler, B. A proline switch explains kinetic heterogeneity in a coupled folding and binding reaction. *Nat. Commun.* **9**, 3332 (2018).
148. Ghosh, J. K. & Ramamoorthi, R. V. *Bayesian Nonparametrics* (Springer, 2003).
149. Pressé, S. & Sgouralis, I. *Data Modeling for the Sciences: Applications, Basics, Computations* (Cambridge Univ. Press, 2023).
150. Hines, K. E., Bankston, J. R. & Aldrich, R. W. Analyzing single-molecule time series via nonparametric Bayesian inference. *Biophys. J.* **108**, 540–556 (2015).
151. Sgouralis, I. & Presse, S. An introduction to infinite HMMs for single-molecule data analysis. *Biophys. J.* **112**, 2021–2029 (2017).
152. Sgouralis, I. et al. A Bayesian nonparametric approach to single molecule Förster resonance energy transfer. *J. Phys. Chem. B* **123**, 675–688 (2019).
153. Saurabh, A. et al. Single-photon smFRET. I: Theory and conceptual basis. *Biophys. Rep.* **3**, 100089 (2023).
154. Jazani, S. et al. An alternative framework for fluorescence correlation spectroscopy. *Nat. Commun.* **10**, 3662 (2019).
155. Gopich, I. V., Kim, J. Y. & Chung, H. S. Analysis of photon trajectories from diffusing single molecules. *J. Chem. Phys.* **159**, 024119 (2023).
156. Meng, F., Kim, J. Y., Gopich, I. V. & Chung, H. S. Single-molecule FRET and molecular diffusion analysis characterize stable oligomers of amyloid-beta 42 of extremely low population. *PNAS Nexus* **2**, pgad253 (2023).
157. Liu, X., Jiang, Y., Cui, Y., Yuan, J. & Fang, X. Deep learning in single-molecule imaging and analysis: recent advances and prospects. *Chem. Sci.* **13**, 11964–11980 (2022).
158. Xu, J. et al. Automated stoichiometry analysis of single-molecule fluorescence imaging traces via deep learning. *J. Am. Chem. Soc.* **141**, 6976–6985 (2019).
159. Thomsen, J. et al. DeepFRET, a software for rapid and automated single-molecule FRET data classification using deep learning. *eLife* **9**, e60404 (2020).
160. Li, J., Zhang, L., Johnson-Buck, A. & Walter, N. G. Automatic classification and segmentation of single-molecule fluorescence time traces with deep learning. *Nat. Commun.* **11**, 5833 (2020).
161. Yuan, J. et al. Analyzing protein dynamics from fluorescence intensity traces using unsupervised deep learning network. *Commun. Biol.* **3**, 669 (2020).
162. Meng, F., Yoo, J. & Chung, H. S. Single-molecule fluorescence imaging and deep learning reveal highly heterogeneous aggregation of amyloid-beta 42. *Proc. Natl Acad. Sci. USA* **119**, e2116736119 (2022).
163. Wanninger, S. et al. Deep-LASI: deep-learning assisted, single-molecule imaging analysis of multi-color DNA origami structures. *Nat. Commun.* **14**, 6564 (2023).
164. Ilieva, N. I., Galvanetto, N., Allegra, M., Brucale, M. & Laio, A. Automatic classification of single-molecule force spectroscopy traces from heterogeneous samples. *Bioinformatics* **36**, 5014–5020 (2020).
165. von Chamier, L. et al. Democratising deep learning for microscopy with ZeroCostDL4Mic. *Nat. Commun.* **12**, 2276 (2021).
166. Bottaro, S. & Lindorff-Larsen, K. Biophysical experiments and biomolecular simulations: a perfect match? *Science* **361**, 355–360 (2018).
167. Piana, S., Klepeis, J. L. & Shaw, D. E. Assessing the accuracy of physical models used in protein-folding simulations: quantitative evidence from long molecular dynamics simulations. *Curr. Opin. Struct. Biol.* **24**, 98–105 (2014).
168. Voelz, V. A., Pande, V. S. & Bowman, G. R. Folding@home: achievements from over 20 years of citizen science herald the exascale era. *Biophys. J.* **122**, 2852–2863 (2023).
169. Chung, H. S., Piana-Agostinetti, S., Shaw, D. E. & Eaton, W. A. Structural origin of slow diffusion in protein folding. *Science* **349**, 1504–1510 (2015).
170. Galvanetto, N. et al. Extreme dynamics in a biomolecular condensate. *Nature* **619**, 876–883 (2023).
171. Best, R. et al. Effect of flexibility and *cis* residues in single molecule FRET studies of polyproline. *Proc. Natl Acad. Sci. USA* **104**, 18964–18969 (2007).
172. Hoefling, M. et al. Structural heterogeneity and quantitative FRET efficiency distributions of polyprolines through a hybrid atomistic simulation and Monte Carlo approach. *PLoS ONE* **6**, e19791 (2011).
173. Pochorovski, I. et al. Experimental and computational study of BODIPY dye-labeled cavitand dynamics. *J. Am. Chem. Soc.* **136**, 2441–2449 (2014).
174. Best, R. B., Hofmann, H., Nettels, D. & Schuler, B. Quantitative interpretation of FRET experiments via molecular simulation: force field and validation. *Biophys. J.* **108**, 2721–2731 (2015).
175. Schröder, G. F., Alexiev, U. & Grubmüller, H. Simulation of fluorescence anisotropy experiments: probing protein dynamics. *Biophys. J.* **89**, 3757–3770 (2005).
176. Grotz, K. K. et al. Dispersion correction alleviates dye stacking of single-stranded DNA and RNA in simulations of single-molecule fluorescence experiments. *J. Phys. Chem. B* **122**, 11626–11639 (2018).
177. Zheng, W., Borgia, A., Borgia, M. B., Schuler, B. & Best, R. B. Empirical optimization of interactions between proteins and chemical denaturants in molecular simulations. *J. Chem. Theory Comput.* **11**, 5543–5553 (2015).
178. Best, R. B. Computational and theoretical advances in studies of intrinsically disordered proteins. *Curr. Opin. Struct. Biol.* **42**, 147–154 (2017).
179. Best, R. B., Zheng, W. & Mittal, J. Balanced protein–water interactions improve properties of disordered proteins and non-specific protein association. *J. Chem. Theory Comput.* **10**, 5113–5124 (2014).
180. Piana, S., Donchev, A. G., Robustelli, P. & Shaw, D. E. Water dispersion interactions strongly influence simulated structural properties of disordered protein States. *J. Phys. Chem. B* **119**, 5113–5123 (2015).
181. Salvi, N., Abyzov, A. & Blackledge, M. Multi-timescale dynamics in intrinsically disordered proteins from NMR relaxation and molecular simulation. *J. Phys. Chem. Lett.* **7**, 2483–2489 (2016).
182. Kummerer, F. et al. Fitting side-chain NMR relaxation data using molecular simulations. *J. Chem. Theory Comput.* **17**, 5262–5275 (2021).
183. Ruff, K. M., Pappu, R. V. & Holehouse, A. S. Conformational preferences and phase behavior of intrinsically disordered low complexity sequences: insights from multiscale simulations. *Curr. Opin. Struct. Biol.* **56**, 1–10 (2019).
184. Papoian, G. A. *Coarse-Grained Modeling of Biomolecules* (CRC Press, 2018).
185. Kim, Y. C. & Hummer, G. Coarse-grained models for simulations of multiprotein complexes: application to ubiquitin binding. *J. Mol. Biol.* **375**, 1416–1433 (2008).
186. Karanicolas, J. & Brooks, C. L. The origins of asymmetry in the folding transition states of protein L and protein G. *Prot. Sci.* **11**, 2351–2361 (2002).
187. Tesei, G., Schulze, T. K., Crehuet, R. & Lindorff-Larsen, K. Accurate model of liquid–liquid phase behavior of intrinsically disordered proteins from optimization of single-chain properties. *Proc. Natl Acad. Sci. USA* **118**, e2111696118 (2021).
188. Heidarsson, P. O. et al. Release of linker histone from the nucleosome driven by polyelectrolyte competition with a disordered protein. *Nat. Chem.* **14**, 224–231 (2022).
189. Zhang, B., Zheng, W., Papoian, G. A. & Wolynes, P. G. Exploring the free energy landscape of nucleosomes. *J. Am. Chem. Soc.* **138**, 8126–8133 (2016).
190. Dannenhoffer-Lafage, T. & Best, R. B. A data-driven hydrophobicity scale for predicting liquid–liquid phase separation of proteins. *J. Phys. Chem. B* **125**, 4046–4056 (2021).
191. Holmstrom, E. D. et al. Accurate transfer efficiencies, distance distributions, and ensembles of unfolded and intrinsically disordered proteins from single-molecule FRET. *Methods Enzymol.* **611**, 287–325 (2018).
192. Holmstrom, E. D., Liu, Z. W., Nettels, D., Best, R. B. & Schuler, B. Disordered RNA chaperones can enhance nucleic acid folding via local charge screening. *Nat. Commun.* **10**, 2453 (2019).
193. Rudzinski, J. E. Recent progress towards chemically-specific coarse-grained simulation models with consistent dynamical properties. *Computation* **7**, 42 (2019).

194. Padding, J. T. & Briels, W. J. Systematic coarse-graining of the dynamics of entangled polymer melts: the road from chemistry to rheology. *J. Phys. Condens. Matter* **23**, 233101 (2011).
195. Cranmer, K., Brehmer, J. & Louppe, G. The frontier of simulation-based inference. *Proc. Natl Acad. Sci. USA* **117**, 30055–30062 (2020).
196. Dingeldein, L., Cossio, P. & Covino, R. Simulation-based inference of single-molecule force spectroscopy. *Mach. Learn. Sci. Technol.* **4**, 025009 (2023).
197. Verdier, H. et al. Simulation-based inference for non-parametric statistical comparison of biomolecule dynamics. *PLoS Comput. Biol.* **19**, e1010088 (2023).
198. Zoldak, G. & Rief, M. Force as a single molecule probe of multidimensional protein energy landscapes. *Curr. Opin. Struct. Biol.* **23**, 48–57 (2013).
199. Hohng, S., Lee, S., Lee, J. & Jo, M. H. Maximizing information content of single-molecule FRET experiments: multi-color FRET and FRET combined with force or torque. *Chem. Soc. Rev.* **43**, 1007–1013 (2014).
200. Wilson, H. & Wang, Q. ABEL-FRET: tether-free single-molecule FRET with hydrodynamic profiling. *Nat. Methods* **18**, 816–820 (2021).
201. Chu, J. et al. Single-molecule fluorescence multiplexing by multi-parameter spectroscopic detection of nanostructured FRET labels. *Nat. Nanotechnol.* https://doi.org/10.1038/s41565-024-01672-8 (2024).
202. Sung, H. L. & Nesbitt, D. J. Ligand-dependent volumetric characterization of manganese riboswitch folding: a high-pressure single-molecule kinetic study. *J. Phys. Chem. B* **126**, 9781–9789 (2022).
203. Patra, S., Anders, C., Erwin, N. & Winter, R. Osmolyte effects on the conformational dynamics of a DNA hairpin at ambient and extreme environmental conditions. *Angew. Chem.* **56**, 5045–5049 (2017).
204. Michalet, X. et al. Development of new photon-counting detectors for single-molecule fluorescence microscopy. *Philos. Trans. R. Soc. Lond. B Biol. Sci.* **368**, 20120035 (2013).
205. Dahmardeh, M., Mirzaalian Dastjerdi, H., Mazal, H., Kostler, H. & Sandoghdar, V. Self-supervised machine learning pushes the sensitivity limit in label-free detection of single proteins below 10 kDa. *Nat. Methods* **20**, 442–447 (2023).
206. Yuan, H. et al. Temperature-cycle microscopy reveals single-molecule conformational heterogeneity. *Phys. Chem. Chem. Phys.* **17**, 6532–6544 (2015).
207. Morales-Inostroza, L. et al. An optofluidic antenna for enhancing the sensitivity of single-emitter measurements. *Nat. Commun.* **15**, 2545 (2023).
208. Budde, J.-H. et al. FRET nanoscopy enables seamless imaging of molecular assemblies with sub-nanometer resolution. Preprint at https://arxiv.org/abs/2108.00024 (2021).
209. Koenig, I. et al. Single-molecule spectroscopy of protein conformational dynamics in live eukaryotic cells. *Nat. Methods* **12**, 773–779 (2015).
210. Terterov, I., Nettels, D., Makarov, D. E. & Hofmann, H. Time-resolved burst variance analysis. *Biophys. Rep.* **3**, 100116 (2023).
211. Vollmar, L., Schimpf, J., Hermann, B. & Hugel, T. Cochaperones convey the energy of ATP hydrolysis for directional action of Hsp90. *Nat. Commun.* **15**, 569 (2024).
212. Song, K. V., Makarov, D. E. & Vouga, E. Compression algorithms reveal memory effects and static disorder in single-molecule trajectories. *Phys. Rev. Res.* **5**, L012026 (2023).
213. Barth, A. et al. Unraveling multi-state molecular dynamics in single-molecule FRET experiments. I. Theory of FRET-lines. *J. Chem. Phys.* **156**, 141501 (2022).
214. Opanasyuk, O. et al. Unraveling multi-state molecular dynamics in single-molecule FRET experiments. II. Quantitative analysis of multi-state kinetic networks. *J. Chem. Phys.* **157**, 031501 (2022).
215. Adhikari, S. & Orrit, M. Progress and perspectives in single-molecule optical spectroscopy. *J. Chem. Phys.* **156**, 160903 (2022).
216. Hwang, H. & Myong, S. Protein induced fluorescence enhancement (PIFE) for probing protein–nucleic acid interactions. *Chem. Soc. Rev.* **43**, 1221–1229 (2014).
217. Ploetz, E. et al. A new twist on PIFE: photoisomerisation-related fluorescence enhancement. *Methods Appl. Fluoresc.* **12**, 012001 (2023).
218. Doose, S., Neuweiler, H. & Sauer, M. Fluorescence quenching by photoinduced electron transfer: a reporter for conformational dynamics of macromolecules. *ChemPhysChem* **10**, 1389–1398 (2009).
219. Haenni, D., Zosel, F., Reymond, L., Nettels, D. & Schuler, B. Intramolecular distances and dynamics from the combined photon statistics of single-molecule FRET and photoinduced electron transfer. *J. Phys. Chem. B* **117**, 13015–13028 (2013).
220. Weisenburger, S. et al. Cryogenic optical localization provides 3D protein structure data with Angstrom resolution. *Nat. Methods* **14**, 141–144 (2017).
221. Gwosch, K. C. et al. MINFLUX nanoscopy delivers 3D multicolor nanometer resolution in cells. *Nat. Methods* **17**, 217–224 (2020).
222. Woll, D. et al. Polymers and single molecule fluorescence spectroscopy, what can we learn? *Chem. Soc. Rev.* **38**, 313–328 (2009).
223. Kalinin, S., Valeri, A., Antonik, M., Felekyan, S. & Seidel, C. A. Detection of structural dynamics by FRET: a photon distribution and fluorescence lifetime analysis of systems with multiple states. *J. Phys. Chem. B* **114**, 7983–7995 (2010).
224. Gopich, I. V. & Szabo, A. Single-molecule FRET with diffusion and conformational dynamics. *J. Phys. Chem. B* **111**, 12925–12932 (2007).
225. Hoffmann, A. et al. Quantifying heterogeneity and conformational dynamics from single molecule FRET of diffusing molecules: recurrence analysis of single particles (RASP). *Phys. Chem. Chem. Phys.* **13**, 1857–1871 (2011).
226. Cario, G. & Franck, J. Über sensibilisierte Fluoreszenz von Gasen. *Z. Phys.* **17**, 202–212 (1923).
227. Kallmann, H. & London, F. Über quantenmechanische Energieübertragungen zwischen atomaren Systemen. *Z. Phys. Chem.* **2**, 207–243 (1928).
228. Perrin, F. Théorie quantique des transferts d'activation entre molécules de méme espèce. Cas des solutions fluorescentes. *Ann. Chim. Phys.* **17**, 283–314 (1932).
229. Andrews, D. L. in *Tutorials in Complex Photonic Media* (eds Noginov, M. A. et al.) (SPIE, 2009).
230. Masters, B. R. Paths to Förster's resonance energy transfer (FRET) theory. *Eur. Phys. J. H* **39**, 87–139 (2014).
231. Oppenheimer, J. R. Minutes of the Pasadena, California, Meeting June 18–20, 1941. *Phys. Rev.* **60**, 158–165 (1941).
232. Arnold, W. & Oppenheimer, J. R. Internal conversion in the photosynthetic mechanism of blue-green algae. *J. Gen. Physiol.* **33**, 423–435 (1950).
233. Förster, T. Energiewanderung und Fluoreszenz. *Naturwissenschaften* **6**, 166–175 (1946).
234. Nelson, P. C. The role of quantum decoherence in FRET. *Biophys. J.* **115**, 167–172 (2018).
235. Olaya-Castro, A. & Scholes, G. D. Energy transfer from Förster–Dexter theory to quantum coherent light-harvesting. *Int. Rev. Phys. Chem.* **30**, 49–77 (2011).
236. Clegg, R. M. in *Reviews in Fluorescence* (eds Geddes, C. D. & Lakowicz, J. R.) Vol. 3, 1–45 (Springer, 2006).
237. Felekyan, S. et al. Full correlation from picoseconds to seconds by time-resolved and time-correlated single photon detection. *Rev. Sci. Instrum.* **76**, 083104 (2005).
238. Viterbi, A. J. Error bounds for convolutional codes and an asymptotically optimum decoding algorithm. *IEEE Trans. Inf. Theory* **13**, 260 (1967).

Acknowledgements
The authors thank R. Covino, S. Gopi, G. Haran, H. Hofmann, E. Lipman, C. Lorenz and D. Makarov for insightful discussions and comments on the manuscript. This work was supported by the Swiss National Science Foundation and the Forschungskredit of the University of Zurich.

Author contributions
All authors contributed to all aspects of this article.

Competing interests
The authors declare no competing interests.

Additional information
Peer review information *Nature Reviews Physics* thanks Nikos Hatzakis, Satyajit Patra and the other, anonymous, reviewer(s) for their contribution to the peer review of this work.

Publisher's note Springer Nature remains neutral with regard to jurisdictional claims in published maps and institutional affiliations.